Inorg. Chem. **2003**, *42*, 796–813

Synthesis and Reactions of Molybdenum Triamidoamine Complexes Containing Hexaisopropylterphenyl Substituents

Dmitry V. Yandulov,[†] Richard R. Schrock,*[,†] Arnold L. Rheingold,[‡] Christopher Ceccarelli,[‡] and William M. Davis[†]

Department of Chemistry, Massachusetts Institute of Technology, Cambridge, Massachusetts 02139, and Department of Chemistry and Biochemistry, University of Delaware, Newark, Delaware 19716

Received August 7, 2002

We have synthesized a triamidoamine ligand ($[(RNCH_2CH_2)_3N]^{3-}$) in which R is 3,5-(2,4,6-i-$Pr_3C_6H_2)_2C_6H_3$ (hexaisopropylterphenyl or HIPT). The reaction between $MoCl_4(THF)_2$ and H_3[HIPTN_3N] in THF followed by 3.1 equiv of $LiN(SiMe_3)_2$ led to formation of orange [HIPTN_3N]MoCl. Reduction of **Mo**Cl (**Mo** = [HIPTN_3N]Mo) with magnesium in THF under dinitrogen led to formation of salts that contain the $\{$**Mo**$(N_2)\}^-$ ion. The $\{$**Mo**$(N_2)\}^-$ ion can be oxidized by zinc chloride to give **Mo**(N_2) or protonated to give **Mo**N═NH. The latter was found to decompose to yield **Mo**H. Other relevant compounds that have been prepared include $\{$**Mo**═N–$NH_2\}^+$ (by protonation of **Mo**N═NH), **Mo**≡N, $\{Mo{=}NH\}^+$ (by protonation of **Mo**≡N), and $\{Mo(NH_3)\}^+$ (by treating **Mo**Cl with ammonia). (The anion is usually $\{B(3,5\text{-}(CF_3)_2C_6H_3)_4\}^- = \{BAr'_4\}^-$.) X-ray studies were carried out on $\{Mg(DME)_3\}_{0.5}$-[**Mo**(N_2)], **Mo**N═NMgBr$(THF)_3$, **Mo**(N_2), **Mo**≡N, and $\{Mo(NH_3)\}\{BAr'_4\}$. These studies suggest that the HIPT substituent on the triamidoamine ligand creates a cavity that stabilizes a variety of complexes that might be encountered in a hypothetical Chatt-like dinitrogen reduction scheme, perhaps largely by protecting against bimolecular decomposition reactions.

Introduction

The discovery of the first dinitrogen complex of a transition metal, $[Ru(NH_3)_5(N_2)]^{2+}$, by Allen and Senoff[1] raised the expectation that eventually it might be possible to activate and reduce dinitrogen to ammonia using a transition metal complex as a catalyst under relatively mild conditions. Such an achievement could lead to a huge savings of energy that is required for the Haber−Bosch process[2,3] and also could help us understand some aspects of how dinitrogen is reduced by various nitrogenases.[4] Tremendous advances have been made in the chemistry of dinitrogen complexes since the discovery of $[Ru(NH_3)_5(N_2)]^{2+}$. Dinitrogen complexes are now known for all metals in groups 4−10 with the exception of palladium and platinum.[5] Dinitrogen most often binds "end-on" to a single metal, but bimetallic μ-N_2 and multimetallic binding modes are also well-documented. Much attention has been given to the "degree of activation" (degree of reduction) of dinitrogen that is possible by two or more metals, and several years ago the ultimate "activation" of dinitrogen was achieved, i.e., splitting of the N≡N bond homolytically by two Mo[N(*t*-Bu)Aryl]$_3$ complexes to give 2 equiv of [N(*t*-Bu)Aryl]$_3$Mo≡N.[6,7] However, Chatt and his group showed that dinitrogen

* To whom correspondence should be addressed. E-mail: rrs@mit.edu.
† Massachusetts Institute of Technology.
‡ University of Delaware.

(1) Allen, A. D.; Senoff, C. V. *J. Chem. Soc., Chem. Commun.* **1965**, 621.
(2) Jenkinson, D. S. *Plant Soil* **2001**, *228*, 3.
(3) Travis, T. *Chem. Ind.* **1993**, 581.
(4) (a) Eady, R. R. *Chem. Rev.* **1996**, *96*, 3013. (b) Eady, R. R. *J. Inorg. Biochem.* **2001**, *86*, 42. (c) Rees, D. C.; Howard, J. B. *Curr. Opin. Chem. Biol.* **2000**, *4*, 559. (d) Rees, D. C.; Chan, M. K.; Kim, J. *Adv. Inorg. Chem.* **1996**, *40*, 89. (e) Burgess, B. K. *Chem. Rev.* **1990**, *90*, 1377. (f) Burgess, B. K.; Lowe, D. J. *Chem. Rev.* **1996**, *96*, 2983.
(5) (a) Fryzuk, M. D.; Johnson, S. A. *Coord. Chem. Rev.* **2000**, *200−202*, 379. (b) Hidai, M.; Mizobe, Y. *Chem. Rev.* **1995**, *95*, 1115. (c) Hidai, M. *Coord. Chem. Rev.* **1999**, *185−186*, 99. (d) Chatt, J.; Dilworth, J. R.; Richards, R. L. *Chem. Rev.* **1978**, *78*, 589. (e) Richards, R. L. *Coord. Chem. Rev.* **1996**, *154*, 83. (f) Richards, R. L. *Pure Appl. Chem.* **1996**, *68*, 1521. (g) Bazhenova, T. A.; Shilov, A. E. *Coord. Chem. Rev.* **1995**, *144*, 69.
(6) Laplaza, C. E.; Cummins, C. C. *Science* **1995**, *268*, 861.
(7) Laplaza, C. E.; Johnson, M. J. A.; Peters, J. C.; Odom, A. L.; Kim, E.; Cummins, C. C.; George, G. N.; Pickering, I. J. *J. Am. Chem. Soc.* **1996**, *118*, 8623.

10.1021/ic020505l CCC: $25.00
Published on Web 01/15/2003

can be protonated in $M(dppe)_2(N_2)_2$ (M = Mo or W) complexes to give 2 equiv of ammonia from one of the two dinitrogens present, the required six electrons presumably coming from a single metal. Therefore, initial "activation" of dinitrogen at multiple metal sites does not appear to be required for ammonia production. However, despite the many successes in transition metal dinitrogen chemistry, reports of catalytic reduction of dinitrogen by protons and a reducing agent are rare.[5,8]

We have been interested in complexes that contain a triamidoamine ligand ($[RN_3N]^{3-} = [(RNCH_2CH_2)_3N]^{3-}$)[9,10] for several reasons: the $[(RNCH_2CH_2)_3N]^{3-}$ ligand is multidentate, the apical site that is created when it binds to a metal is sterically protected by the three amido substituents, and the metal to which such a ligand is coordinated is likely to be in an oxidation state of 3+ or greater. In view of the presence of molybdenum in one of the nitrogenases,[4,5] we have focused on the synthesis and study of molybdenum complexes that contain triamidoamine ligands for the reduction of dinitrogen. We have shown that Mo species in which R = $SiMe_3$[11] or C_6F_5[12] are poised for binding and reducing dinitrogen to yield $\{[RN_3N]MoN{=}N\}^-$ complexes. However, various problems have been encountered when R = TMS or C_6F_5, among them serious side reactions such as Si migrations, or what we suspect to be CF reactions at the ortho position in pentafluorophenyl complexes. We also were not encouraged by the potential of such systems for the reduction of dinitrogen with protons and electrons. Therefore, we turned to the molybdenum triamidoamine complexes that contain ordinary aryl groups (e.g., Ar = C_6H_5, 4-FC_6H_4, 4-*t*-BuC_6H_4, and 3,5-$Me_2C_6H_3$).[13] We found that $[ArN_3N]MoCl$ species could not be prepared when the aryl group contained one or more ortho substituents, presumably because of steric problems at some crucial stage in the synthesis. Reduction of $[ArN_3N]MoCl$ complexes under dinitrogen with sodium amalgam yielded complexes of the type $[ArN_3N]MoN{=}NMo[ArN_3N]$, while two electron reduction (with sodium naphthalenide) yielded $\{[ArN_3N]MoN{=}N\}^-$ derivatives. Since $[RN_3N]MoN{=}NMo[RN_3N]$ complexes have proven to be relatively stable toward protonation of dinitrogen before the complex is destroyed, they become reaction "sinks" unless they can be reduced under dinitrogen by 2e to give 2 equiv of $\{[ArN_3N]MoN{=}N\}^-$ species, a reaction that has been observed when Ar = pentafluorophenyl[12] but one that does not involve N−N splitting. The X-ray structure of $\{[t\text{-}BuC_6H_4N_3N]Mo\}_2(\mu\text{-}N_2)$ revealed a tightly interdigitated set of six *t*-BuC_6H_4 groups at the two ends of the MoN=NMo core, a fact that suggested that $\{[3,5\text{-}Ph_2C_6H_3N_3N]Mo\}_2(\mu\text{-}N_2)$, a *meta*-terphenyl-substituted species, would be unlikely to form for steric reasons. This proposal was supported by preliminary electrochemical studies.[13c] We also were pleased to find that methylation of $[ArN_3N]MoN{=}NR$ complexes (R = $SiMe_3$ or Me) yielded $\{[ArN_3N]MoN{=}NMe_2\}^+$ species cleanly, with no significant side reactions taking place at the ligand's amido nitrogens. Therefore, we became interested in preparing molybdenum complexes that contain even more crowded *meta*-terphenyl-substituted ligands in the hope that we could essentially eliminate bimolecular chemistry. It is this interest that directed us toward triamidoamine ligands substituted with the 3,5-(2,4,6-i-$Pr_3C_6H_2)_2C_6H_3$ (or HIPT = hexaisopropylterphenyl) group. In this paper we report the full details of the syntheses and structures of several such complexes that contain a ligand in the apical position that is either dinitrogen itself or one that could be derived from dinitrogen in a hypothetical Chatt-like reduction process. A preliminary account of this work has been published.[14]

Results and Discussion

Synthesis of $H_3[HIPTN_3N]$ and MoCl. The Hart reaction[15] between iodo-2,4,6-tribromobenzene and 3.5 equiv of triisopropylphenylmagnesium bromide afforded HIPTBr (eq 1) in moderate yield as a white crystalline solid that could be isolated by crystallization from pentane. The reaction was carried out in the presence of excess magnesium, which resulted in conversion of the TripI formed in the "double aryne" reaction to the corresponding Grignard reagent. Subsequent hydrolysis then produced HIPTBr and triisopropylbenzene, which facilitated isolation of the HIPTBr.

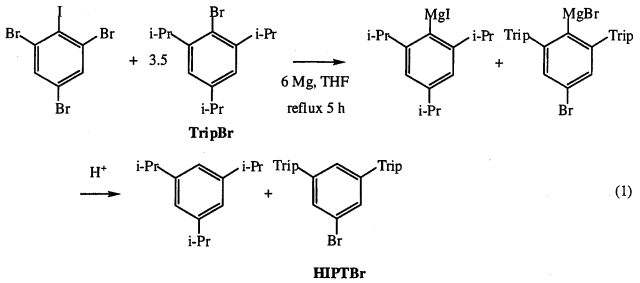

Palladium-catalyzed coupling[16,17] between 3.05 equiv of HIPTBr and triethylenetetramine in the presence of NaO-*t*-Bu (eq 2) proceeded smoothly in toluene at 80 °C over a period of 20 h to give $H_3[HIPTN_3N]$ in good yield. No significant "overarylated" product (containing a doubly arylated amine) was observed, presumably because of the bulky nature of the HIPT group. (Overarylation was observed with small aryl groups.[13b,c]) Purification of $H_3[HIPTN_3N]$ therefore was greatly simplified. Although $H_3[HIPTN_3N]$ has

(8) (a) Dickson, C. R.; Nozik, A. J. *J. Am. Chem. Soc.* **1978**, *100*, 8007. (b) Yu, M.; Didenko, L. P.; Kachapina, L. M.; Shilov, A. E.; Shilova, A. K.; Struchkov, Y. T. *J. Chem. Soc., Chem. Commun.* **1989**, 1467. (c) Dziegielewski, J. O.; Grzybek, R. *Polyhedron* **1990**, *9*, 645. (d) Shilov, A. E. *J. Mol. Catal.* **1987**, *41*, 221. (d) Komori, K.; Oshita, H.; Mizobe, Y.; Hidai, M. *J. Am. Chem. Soc.* **1989**, *111*, 1939. (e) Tanaka, K.; Hozumi, Y.; Tanaka. *Chem. Lett.* **1982**, 1203.
(9) Schrock, R. R. *Acc. Chem. Res.* **1997**, *30*, 9.
(10) Schrock, R. R. *Pure Appl. Chem.* **1997**, *69*, 2197.
(11) (a) O'Donoghue, M. B.; Zanetti, N. C.; Schrock, R. R.; Davis, W. M. *J. Am. Chem. Soc.* **1997**, *119*, 2753. (b) O'Donoghue, M. B.; Davis, W. M.; Schrock, R. R. *Inorg. Chem.* **1998**, *37*, 5149. (c) O'Donoghue, M. B.; Davis, W. M.; Schrock, R. R.; Reiff, W. M. *Inorg. Chem.* **1999**, *38*, 243.
(12) Kol, M.; Schrock, R. R.; Kempe, R.; Davis, W. M. *J. Am. Chem. Soc.* **1994**, *116*, 4382.
(13) (a) Greco, G. E.; Popa, A. I.; Schrock, R. R. *Organometallics* **1998**, *17*, 5591. (b) Greco, G. E.; Schrock, R. R. *Inorg. Chem.* **2001**, *40*, 3850. (c) Greco, G. E.; Schrock, R. R. *Inorg. Chem.* **2001**, *40*, 3860.
(14) Yandulov, D. V.; Schrock, R. R. *J. Am. Chem. Soc.* **2002**, *124*, 6252.
(15) Du, C. J. F.; Hart, H.; Ng, K. K. D. *J. Org. Chem.* **1986**, *51*, 3162.
(16) Wolfe, J. P.; Buchwald, S. L. *J. Org. Chem.* **2000**, *65*, 1144.
(17) Hartwig, J. F. *Angew. Chem., Int. Ed.* **1998**, *37*, 2046.

not yet been obtained in crystalline form, the amorphous material analyzed well and was found to be of acceptable quality for subsequent synthesis of molybdenum complexes.

$$1/3(H_2NCH_2CH_2)_3N + HIPTBr \xrightarrow[\substack{1.5\%\ rac\text{-BINAP}\\ 1.4NaO\text{-}t\text{-Bu, toluene,}\\ 80\ ^\circ C,\ 20\ h}]{0.5\%\ Pd_2(dba)_2} 1/3(HIPTNHCH_2CH_2)_3N \quad (2)$$

The reaction between $MoCl_4(THF)_2$ and $H_3[HIPTN_3N]$ in THF produced a dark red solution in 1 h that we assume to contain an adduct,[13a,b] the exact nature of which is not known. Addition of 3.1 equiv of $LiN(SiMe_3)_2$ over a period of 30 min to this red solution led to formation of orange $[HIPTN_3N]$-MoCl (**Mo**Cl). A successful strategy for the high-yield synthesis of $[RN_3N]MCl$ complexes developed for $R = C_6F_5$ and other aryl-substituted triamidoamine ligands consisted of addition of NEt_3 to the initially formed adduct.[12] That strategy did not work when the aryl was an ordinary phenyl group; LiMe and MeMgCl were found to be necessary to dehydrohalogenate the presumably less acidic adducts.[13b] Lithiation of $H_3[HIPTN_3N]$ with butyllithium in toluene or pentane afforded $Li_3[HIPTN_3N]$ as a white, amorphous, and extremely air-sensitive solid. However, addition of Li_3-$[HIPTN_3N]$ to either $MoCl_4(THF)_2$ or $MoCl_3(THF)_3$ under a variety of conditions typically gave only a small amount of **Mo**Cl, identified by its characteristic paramagnetically shifted backbone ^1H NMR resonances, and, in several cases, a trace amount of **Mo**N_2 (vide infra).

MoCl is a red-orange crystalline solid that can be isolated by crystallization from pentane. Like most other compounds described here, it is extremely sensitive to air and moisture. Proton NMR spectra of **Mo**Cl are closely analogous to those obtained for a number of other $[ArN_3N]MoCl$ complexes.[13b,c] As found for all paramagnetic complexes described here, protons in the isopropyl groups in the para position of the triisopropylphenyl (Trip) rings and the meta protons appear in the ^1H NMR spectra as relatively sharp resonances with typical diamagnetic chemical shifts, and the former reveal J_{HH} coupling. However, the diastereotopic methyl groups of the isopropyl groups in the 2 and 6 positions of the Trip rings always appear as broad singlets with different line widths. Since these resonances appear as sharp doublets of identical line widths in closely related diamagnetic Mo derivatives, the difference in the line widths of the isopropyl methyl groups in the 2 and 6 positions seen in the case of **Mo**Cl and other paramagnetic species is likely due to a greater proximity of one of the methyl groups to the paramagnetic metal center (on the average) rather than to hindered rotation of the *meta*-terphenyl substituents around N−C bonds.

Reduction of MoCl under N_2. Preparation of $[Bu_4N]$-{$[HIPTN_3N]MoN{=}N$} and $[HIPTN_3N]MoN_2$. Reduction of **Mo**Cl with 10 equiv of magnesium powder in THF or DME under a dinitrogen atmosphere results in a dramatic color change from red-orange to dark green. Activation of the magnesium is essential for a practical reaction rate and can be accomplished by either vigorously stirring the heterogeneous mixture or preferentially by treating the magnesium with ~0.5 equiv of 1,2-dibromoethane or 1,2-dichloroethane (per Mo) prior to addition of **Mo**Cl. Activation with 1,2-dichloroethane is required in some cases, in view of the possibility of otherwise incorporating both bromide and/or chloride in some of the products (vide infra). With proper activation of magnesium in THF, full reduction of **Mo**Cl is possible in less than 30 min. According to its IR spectrum, the dark green solution obtained upon reduction of **Mo**Cl with magnesium in THF under dinitrogen contained **Mo**N═NMgCl$(THF)_3$ in equilibrium with various {$[HIPTN_3N]$-MoN═N}$^-$ ($[$**Mo**$N_2]^-$) salts. These compounds are discussed in detail in a later section.

When reduction of **Mo**Cl with magnesium in THF was followed by addition of dioxane (10 equiv/Mo) and Bu_4NCl and the reaction was stirred overnight, the solution IR spectrum of the reaction mixture showed presence of only $[$**Mo**$N_2]^-$. Subsequent extraction of the reaction mixture with benzene led to isolation of emerald-green, diamagnetic $[Bu_4N][$**Mo**$N_2]$ as an amorphous solid in 82% yield. An IR spectrum of $[Bu_4N][$**Mo**$N_2]$ in C_6D_6 revealed a ν_{NN} stretch at 1855 cm^{-1}; in THF it was found at 1859 cm^{-1}. The $^{15}N_2$ analogue was isolated in 90% yield (~1.5 g) by a procedure under $^{15}N_2$ that was analogous to that used for the synthesis of the unlabeled complex. In $[Bu_4N][$**Mo**$^{15}N_2]$ $\nu_{^{15}N^{15}N}$ was found at 1794 cm^{-1} in C_6D_6. The ^{15}N NMR spectrum of $[Bu_4N][$**Mo**$^{15}N_2]$ in C_6D_6 features two broad resonances at 381 and 367 ppm that can be ascribed to N_α and N_β, respectively, in the dinitrogen ligand. We ascribe the broadening of these resonances, and resonances in the ^1H NMR spectrum, at least partly to the presence of paramagnetic **Mo**N_2 (vide infra) as an impurity and an interconversion of $[Bu_4N][$**Mo**$N_2]$ and $[$**Mo**$N_2]$ at a rate of the order of the NMR time scale. Since $[Bu_4N][$**Mo**$N_2]$ is a strong reductant (it reacts readily even with Teflon), formation of trace amounts of **Mo**N_2 is virtually impossible to avoid.

The dinitrogen complex **Mo**N_2 can be prepared by adding zinc chloride to a filtered dark green solution obtained by reduction of **Mo**Cl by magnesium in THF. Addition of zinc chloride resulted in a rapid color change from green to brown and formation of a gray precipitate of zinc metal. After 30 min the volatile components of the reaction mixture were removed and the green-brown residue was recrystallized from pentane to yield paramagnetic, green-brown **Mo**N_2 in 80% yield. The complex is highly soluble in pentane but can be recrystallized efficiently from Me_4Si on a small scale. The $^{15}N_2$ analogue was prepared similarly from $[Bu_4N][$**Mo**$^{15}N_2]$. In **Mo**N_2 $\nu_{NN} = 1990$ cm^{-1} (in C_6D_6), while in **Mo**$^{15}N_2$ $\nu_{^{15}N^{15}N} = 1924$ cm^{-1}. The ^1H NMR spectrum of **Mo**N_2 in C_6D_6 features two paramagnetically shifted resonances at 23.2 and −33.5 ppm, similar to those observed for the methylene backbone protons of $[TMSN_3N]MoN_2$ (14.0 and −40.6 ppm).[11b] Therefore, we presume that **Mo**N_2, like its $[TMSN_3N]^{3-}$ analogue, is a low-spin d^3 species. **Mo**N_2 reacts with C_6D_5Cl when it is employed as a solvent over a period of days (~25% conversion after 2 days) to give **Mo**Cl. In contrast, **Mo**N_2 appears to be relatively stable in C_6H_5F. The

structure of **Mo**N_2 was confirmed in an X-ray study (see later section).

When **Mo**$^{15}N_2$ is placed in C_6D_6 solution under a large excess (~40 equiv) of $^{14}N_2$, $^{14}N_2$ was found to exchange with coordinated $^{15}N_2$ over a period of 1−2 days at 22 °C. The exchange can be followed readily by IR and was shown to proceed at a rate that is first order in Mo with $t_{1/2} \sim 35$ h at 22 °C. This rate of exchange is considerably faster than the rate of exchange in [TMSN_3N]MoN_2 (days at 22 °C),[11b] which is consistent with the stronger back-bonding to dinitrogen in [TMSN_3N]MoN_2 (ν_{NN} = 1934 cm^{-1} in pentane)[11b] versus **Mo**N_2 (1990 cm^{-1}). We propose that the intermediate in the exchange reaction is trigonal monopyramidal [HIPTN_3N]Mo. Although trigonal monopyramidal [TMSN_3N]M complexes where M is a first row metal (Ti − Fe) are known,[18] to our knowledge no trigonal monopyramidal triamidoamine complex that contains a second or a third row metal has been observed.

A proton NMR spectrum of equal amounts of MoN_2 and [Bu_4N][**Mo**N_2] in C_6D_6 at 22 °C showed broadened resonances for **Mo**N_2 at 23 ppm (NCH_2), −4.8 ppm (*o*-C*H*), and −33 ppm (NCH_2) and a single set of exchange-averaged resonances in the diamagnetic region, while the backbone NCH_2, *o*-C*H*, and *p*-C*H* resonances for [Bu_4N][**Mo**N_2] could not be observed. We propose that at this temperature the Bu_4N^+ cation and one electron are moving from [Bu_4N]-[**Mo**N_2] to **Mo**N_2 at a rate close to or faster than the NMR time scale. Interconversion of [Bu_4N][**Mo**N_2] and traces of **Mo**N_2 is believed to be at least partly responsible for the characteristic broadening of the NMR resonances of [Bu_4N]-[**Mo**N_2] and slight variation of the chemical shifts observed in different batches of [Bu_4N][**Mo**N_2].

One sample of [Bu_4N][**Mo**$^{15}N_2$] in C_6D_6 underwent a slow exchange ($t_{1/2} \sim 63$ days) with atmospheric $^{14}N_2$ (~13 mM in C_6D_6 in contact with ~10 equiv of $^{14}N_2$ in a closed system). With time, a trace of **Mo**N_2 appeared (according to IR spectra), from ~1.7 to 2.5% of all Mo complexes present. Since exchange of **Mo**N_2 with [Bu_4N][**Mo**N_2] is fast on the chemical time scale, it is not surprising that the ratio of **Mo**$^{15}N_2$ to **Mo**$^{14}N_2$ (4.3) and the ratio of [Bu_4N][**Mo**$^{15}N_2$] to [Bu_4N][**Mo**$^{14}N_2$] (4.2) are nearly the same with time; i.e., the distribution of $^{15}N_2$ in [Bu_4N][**Mo**N_2] is mirrored in **Mo**N_2 through fast intermolecular transfer of $[Bu_4N]^+$ and an electron. Since the rate of $^{14}N_2/^{15}N_2$ exchange in **Mo**N_2 is considerably faster than in a sample of [Bu_4N][**Mo**$^{15}N_2$], we believe that the $^{14}N_2/^{15}N_2$ exchange observed for [Bu_4N]-[**Mo**$^{15}N_2$] takes place partly, if not completely, in **Mo**N_2 rather than in [Bu_4N][**Mo**$^{15}N_2$].

Elucidation of the Nature of Magnesium Diazenides. Extraction of the crude product obtained upon reduction of **Mo**Cl with 10 equiv of Mg under dinitrogen in THF with pentane yields purple-red, diamagnetic **Mo**N═NMgCl(THF)$_3$ (eq 3). (When the Mg was activated with 1,2-dibromoethane, the product was **Mo**N═NMgBr(THF)$_3$, as was confirmed in an X-ray study; see later section.) The yield of **Mo**N═NMgCl(THF)$_3$ (49%) appears to be limited by the compound's high solubility in pentane. In contrast to [Bu_4N]-[**Mo**N_2], the Mg derivative does not readily interconvert with the **Mo**N_2 impurity in C_6D_6 at 22 °C; the resonances in ^{15}N and ^1H NMR spectra therefore are relatively sharp. The $^{15}N_2$ analogue was isolated in 39% yield in an analogous reaction under $^{15}N_2$ (~4.5 equiv/Mo). Availability of both compounds as analytically pure solids has allowed us to understand the complex IR patterns observed for **Mo**N═NMgCl(THF)$_3$ and to gain a better understanding of the dissociation equilibria taking place in solution.

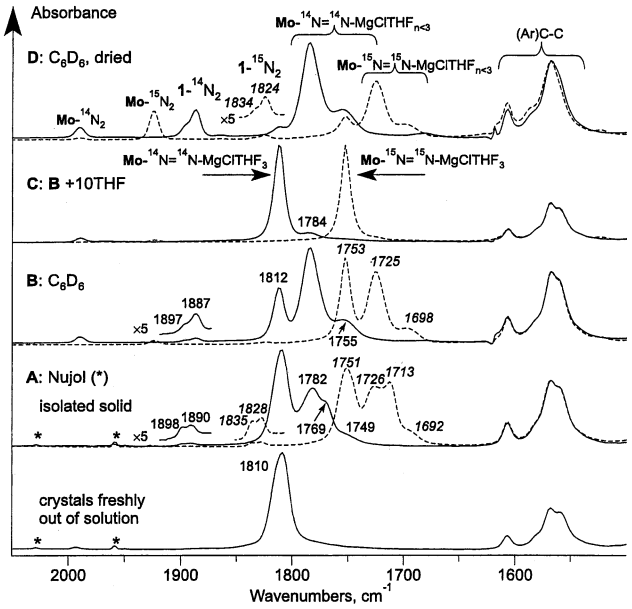

Figure 1. IR spectra of **Mo**N_2MgCl(THF)$_3$ (—, $\nu_{^{14}N-^{14}N}$, cm^{-1}, regular font) and **Mo**$^{15}N_2$MgCl(THF)$_3$ (---, $\nu_{^{15}N-^{15}N}$, cm^{-1}, italic font) in Nujol (A), in C_6D_6 (B, 13 mM ($^{14}N_2$) and 42 mM ($^{15}N_2$)), in C_6D_6 with 10 equiv of THF (C; THF was added to the solutions used to obtain the spectra in (B)), and in C_6D_6 following drying of the solids at 80 °C for 2−3 h (D). All C_6D_6 spectra were obtained by subtracting the solvent spectrum.

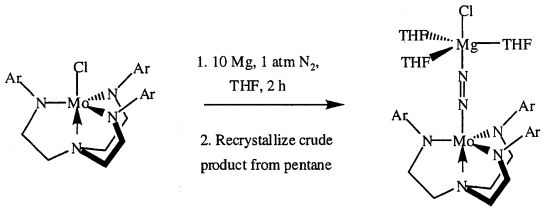

(3)

The IR spectrum of isolated **Mo**N═NMgCl(THF)$_3$ in Nujol (Figure 1A) is complex, featuring at least six ν_{NN} bands with a major band at 1810 cm^{-1}. All bands are shifted by ~60 cm^{-1} in the spectrum of **Mo**^{15}N═^{15}NMgCl(THF)$_3$, which suggests that they can all be attributed to a stretching mode involving dinitrogen. In C_6D_6 (part B), a similar pattern is observed, but the major band is now that at 1784 cm^{-1}. A proton NMR spectrum of this sample reveals that ~3 equiv of THF is present per Mo. Addition of 10 equiv of THF to part B strongly enhances the band at 1812 cm^{-1} (part C), while drying the solid diminishes the intensity of the 1812 cm^{-1} band relative to other bands (part D; ~1.3 equiv of THF is present by ^1H NMR). The spectra in Figure 1 also feature ν_{NN} bands of **Mo**N_2 and **Mo**$^{15}N_2$ that typically amount

(18) Cummins, C. C.; Lee, J.; Schrock, R. R. *Angew. Chem., Int. Ed. Engl.* **1992**, *31*, 1501.

to ~5% of all observable Mo species as a consequence of the susceptibility of **Mo**N═NMgCl(THF)$_3$ toward oxidation.

We assign the major band in Nujol at 1810 cm^{-1} and the corresponding band at 1812 cm^{-1} in C_6D_6 to **Mo**N═NMgCl(THF)$_3$, i.e., the species in which magnesium is coordinated to N_β and three molecules of THF are bound to the magnesium, since a Nujol IR spectrum of the crystals of **Mo**N═NMgCl(THF)$_3$ freshly taken out of solution (Figure 1A) shows only the band at 1810 cm^{-1}, and three THF molecules were found bound to Mg in the X-ray study of the **Mo**N═NMgBr(THF)$_3$ analogue (vide infra). We attribute the spectral changes induced upon addition of a large excess of THF, or by drying the solid, to a shifting of the equilibrium between **Mo**N═NMgCl(THF)$_3$ (at 1810 cm^{-1} in Nujol and 1812 cm^{-1} in C_6D_6) and **Mo**N═NMgCl(THF)$_{n<3}$ (1782, 1769, and 1749 cm^{-1} in Nujol; 1784, 1755 cm^{-1} in C_6D_6). Assignment of the lower frequency bands to **Mo**N═NMgCl(THF)$_{n<3}$ species is consistent with a progressively stronger Mg−N_β bond, as would be expected for an increasingly desolvated magnesium center. It is also possible that loss of THF results in some π-coordination of the Trip rings to magnesium.[19] Dimerization of **Mo**N═NMgCl(THF)$_{n<3}$ species to yield Mg$_2$(μ-Cl)$_2$ dimers also cannot be ruled out.

The weak ν_{NN} bands at 1898 and 1890 cm^{-1} in Nujol (1897 and 1887 cm^{-1} in C_6D_6 in the $^{14}N_2$ species) grow in intensity upon decreasing the amount of THF present (cf. parts C, B, and D in Figure 1), but they cannot correspond to **Mo**N═NMgCl(THF)$_{n<3}$, since they are shifted to higher energies by 75−88 cm^{-1} compared to **Mo**N═NMgCl(THF)$_3$. In fact, these C_6D_6 values are higher than that of the free anion [**Mo**N_2]$^-$ in C_6D_6 (1855 cm^{-1}) but they are lower than that of **Mo**N_2 (1990 cm^{-1}). Therefore we propose that the 1897 and 1887 cm^{-1} bands correspond to a "zwitterionic" form in which a [MgCl(THF)$_x$]$^+$ cation (x unknown) is bound to the equatorial amide nitrogens (**1**). Binding of the Lewis acid to the amide nitrogens should make the Mo center less electron rich and consequently lead to an increase of ν_{NN} from that of free [**Mo**N_2]$^-$. Such an effect on the ν_{NN} is fully analogous to that observed by Sellmann in studies of protonation/alkylation of auxiliary thiolate ligands in iron carbonyl derivatives.[20]

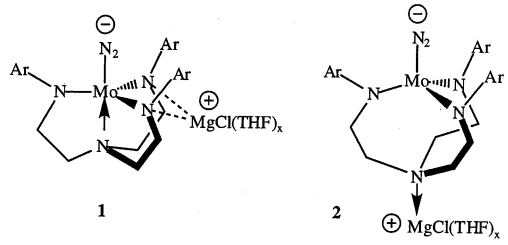

A similar effect on ν_{NN} might be anticipated for the structure in which the magnesium rather than Mo is bound to the inverted amine donor (**2**). However, since the cation in **2** would be located 5 σ bonds away from Mo, we expect that the general charge effect would be minimal in structure

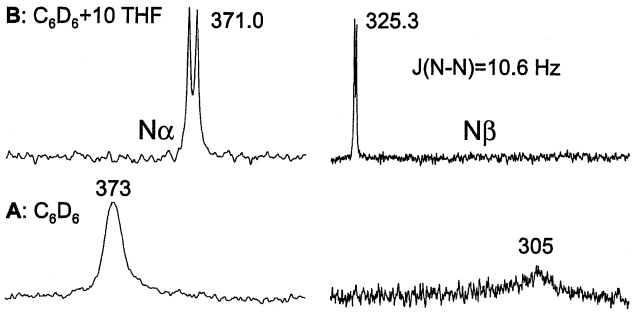

Figure 2. ^{15}N NMR spectra of **Mo**$^{15}N_2$MgCl(THF)$_3$ in C_6D_6 (42 mM, A) and in C_6D_6 with 10 equiv of THF added (42 mM, B) with chemical shifts in ppm vs NH_3. These solutions (A and B) were used to obtain IR spectra B and C, respectively, in Figure 1.

2 and that the net result of this binding mode would be fully analogous to that of simply dissociating the amine ligand. The ν_{NN} frequency in hypothetical Mo(N_2)(NH_2)$_3$ was computed to be 42 cm^{-1} *lower* than that of Mo(N_2)(NH_2)$_3$-(NH_3) (both in their doublet ground states);[21] i.e., dissociation of a ligand trans to the N_2 ligand should cause ν_{NN} to *decrease*. Since ν_{NN} in the free anion is found at 1855 cm^{-1}, structure **2** therefore cannot explain the shift to higher frequencies at 1897 and 1887 cm^{-1} in C_6D_6. The possibility of simultaneously binding more than one {MgL$_n$}$^+$ unit to [**Mo**N_2]$^-$ to give cationic species responsible for the IR bands assigned to **1** seems unlikely, as that would produce free [**Mo**N_2]$^-$, which is not observed in any of the spectra in Figure 1. Although oxidation of Mg diazenides by adventitious impurities could yield the extra {MgL$_n$}$^+$, along with **Mo**N_2, comparison of the spectra in Figure 1D shows that intensities of the bands assigned to **1** do not parallel intensities of bands due to **Mo**N_2. Since we will also show later that interaction of **Mo**N_2 with Brønsted acids results in a shift of the ν_{NN} band at 1990 cm^{-1} to higher frequencies, the 1897 and 1887 cm^{-1} bands are unlikely to result from an interaction of magnesium electrophile(s) with **Mo**N_2.

The proposed equilibria taking place in C_6D_6 solutions of **Mo**N═NMgCl(THF)$_3$, namely partial loss of THF bound to magnesium and multiple-site binding of {MgCl(THF)$_x$}$^+$, also affect the ^{15}N NMR spectra of **Mo**^{15}N═^{15}NMgCl(THF)$_3$ (Figure 2). In the absence of additional THF (part A), the N_β resonance is found at ~305 ppm and is nearly broadened into the baseline, and broadening of the N_α resonance at 373 ppm is also observed. According to the IR spectrum B in Figure 1, the A solution contains comparable amounts of **Mo**^{15}N═^{15}NMgCl(THF)$_3$ and the species assigned as **Mo**^{15}N═^{15}NMgCl(THF)$_{n<3}$. Addition of 10 equiv of THF to this solution shifts the equilibrium nearly completely toward **Mo**^{15}N═^{15}NMgCl(THF)$_3$ (Figure 1C), and the ^{15}N NMR spectrum now displays two sharp doublets at 371.0 (N_α) and 325.3 ppm (N_β; Figure 2B). Some sharpening of resonances is also seen in the ^{1}H NMR spectrum. It is notable that the N_β resonance shifts downfield by 20 ppm in spectrum B as the equilibrium mixture of **Mo**^{15}N═^{15}NMgCl(THF)$_3$ and **Mo**^{15}N═^{15}NMgCl(THF)$_{n<3}$ is transformed into a mixture that contains largely **Mo**^{15}N═^{15}NMgCl(THF)$_3$. This shift is

(19) Robinson, G. H. *Acc. Chem. Res.* **1999**, *32*, 773.
(20) Sellmann, D.; Sutter, J. *Acc. Chem. Res.* **1997**, *30*, 460.
(21) Khoroshun, D. V.; Musaev, D. G.; Morokuma, K. *Mol. Phys.* **2002**, *100*, 523.

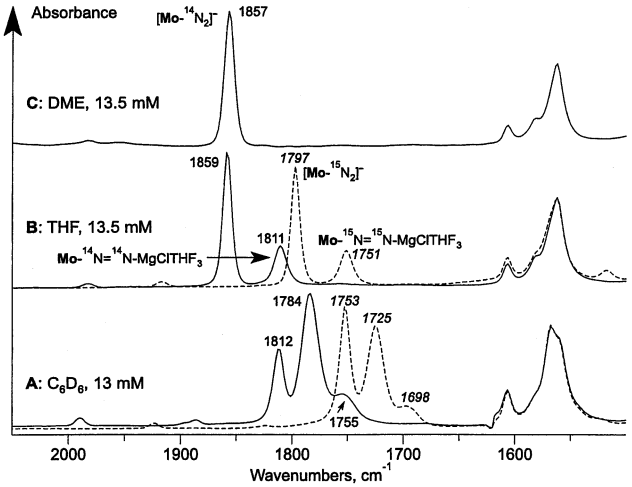

Figure 3. IR spectra of **Mo**N=NMgCl(THF)$_3$ (—, $\nu_{^{14}N-^{14}N}$, cm^{-1}, regular font) and **Mo**^{15}N$_2$MgClTHF$_3$ (---, $\nu_{^{15}N-^{15}N}$, cm^{-1}, italic font) in C_6D_6 (A), in THF (B), and in DME (C) with solvent spectra subtracted.

consistent with stronger {Mg}···N$_\beta$ interactions in **Mo**^{15}N=^{15}NMgCl(THF)$_{n<3}$ than in **Mo**^{15}N=^{15}NMgCl(THF)$_3$, since the ^{15}N NMR resonance of N$_\beta$ in free [**Mo**N$_2$]$^-$ is shifted even further downfield, to 367 ppm (vide supra).

Dissociation of Magnesium from MoN=NMgCl(THF)$_3$. Isolated red-purple **Mo**N=NMgCl(THF)$_3$ forms dark green solutions in THF or DME, which, according to the IR spectra in Figure 3, contain predominantly free [**Mo**N$_2$]$^-$, in addition to **Mo**N=NMgCl(THF)$_3$. (Spectrum 3B is closely analogous to that recorded on a solution of reduced **Mo**Cl.) These observations indicate that **Mo**N=NMgCl(THF)$_3$ reversibly dissociates into [**Mo**N$_2$]$^-$ and {MgCl$_n$L$_m$}$^{(2-n)+}$ ions in neat THF or DME (eq 4) and that this dissociation is considerably more pronounced in DME than in THF (cf. parts B and C in Figure 3).

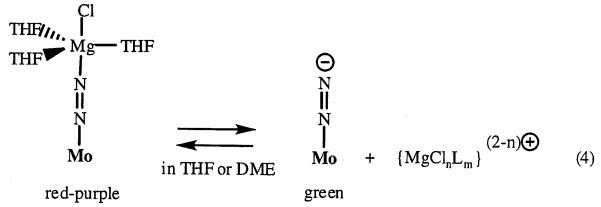

Although the equilibrium ratio of the integrated IR absorbances {*A*([**Mo**N$_2$]$^-$)/*A*(**Mo**N$_2$MgCl(THF)$_3$)} in part B decreases with increasing concentration, these changes do not correspond to those expected for the simplest equilibrium shown in eq 5. We suspect that the dissociation process consists of a series of coupled equilibria, in which [MgCl(THF)$_5$]$^+$ disproportionates into MgCl$_2$(THF)$_4$, [Mg(THF)$_6$]$^{2+}$, [MgCl$_4$]$^{2-}$, and [Mg$_2$(μ-Cl)$_3$(THF)$_6$]$^+$ [22,23] and [**Mo**N$_2$]$^-$ possibly binds [Mg(THF)$_n$]$^{2+}$ at N$_\beta$ (vide infra). Interestingly, addition of increasing amounts of [Bu$_4$N][**Mo**N$_2$] to a THF solution of **Mo**N=NMgCl(THF)$_3$ leads to a *decrease* in the amount of **Mo**N=NMgCl(THF)$_3$; i.e., [Bu$_4$N][**Mo**N$_2$] *promotes* dissociation of **Mo**N=NMgCl(THF)$_3$ into [**Mo**N$_2$]$^-$ and {MgCl$_n$L$_m$}$^{(2-n)+}$. Since it is known[22,23] that [Bu$_4$N][BF$_4$] converts MgCl$_2$(THF)$_2$ into [Bu$_4$N]$_2$[MgCl$_4$] and [Mg(THF)$_6$][BF$_4$]$_2$, the unexpected effect of [Bu$_4$N][**Mo**N$_2$] on the process of dissociation of magnesium can be explained as shown in eq 6. In effect, Bu$_4$N$^+$ helps sequester Cl$^-$ as [MgCl$_4$]$^{2-}$, causing a net decrease in the amount of **Mo**N=NMgCl(THF)$_3$, despite the opposing influence of increasing the concentration of [**Mo**N$_2$]$^-$.

(22) Sobota, P.; Duda, B. *J. Organomet. Chem.* **1987**, *332*, 239 and references therein.
(23) Sobota, P.; Pluzinski, T.; Utko, J.; Lis, T. *Inorg. Chem.* **1989**, *28*, 2217.

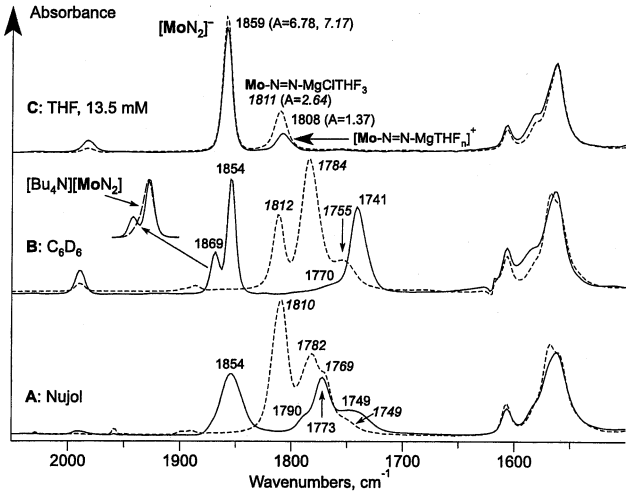

Figure 4. IR spectra of [Mg(DME)$_3$]$_{0.5}$[**Mo**N$_2$] (—, ν_{N-N}, cm^{-1}, regular font) and **Mo**N=NMgClTHF$_3$ (---, ν_{N-N}, cm^{-1}, italic font) in Nujol (A), in C_6D_6 (B), and in THF (C) with solvent spectra subtracted. The inset in (B) compares [**Mo**N$_2$]$^-$ ν_{N-N} bands in [Bu$_4$N][**Mo**N$_2$] and [Mg(DME)$_3$]$_{0.5}$[**Mo**N$_2$].

$$\mathbf{Mo}N{=}NMgCl(THF)_3 + 2THF \rightleftharpoons [\mathbf{Mo}N_2]^- + [MgCl(THF)_5]^+ \quad (5)$$

$$2[Bu_4N][\mathbf{Mo}N_2]^- + 4\mathbf{Mo}N{=}NMgCl(THF)_3 + 6THF \rightarrow 6[\mathbf{Mo}N_2]^- + [Bu_4N]_2[MgCl_4] + 3[Mg(THF)_6]^{2+} \quad (6)$$

Reduction of [HIPTN$_3$N]MoCl in Dimethoxyethane. Reduction of **Mo**N$_2$ with magnesium in DME affords, after crystallization from a mixture of DME and pentane, a dark forest-green crystalline solid with the composition [Mg(DME)$_3$]$_{0.5}$[**Mo**N$_2$], in 69% yield, according to elemental analysis. (No chloride was found.) The IR spectrum of the solid in Nujol (Figure 4A) features comparable amounts of free [**Mo**N$_2$]$^-$ (1854 cm^{-1}) and species assigned as [**Mo**N=NMg(DME)$_n$]$^+$ (1790, 1773, 1749 cm^{-1}). [Mg(DME)$_3$]$_{0.5}$[**Mo**N$_2$] is soluble in benzene (to give a dark red-green solution), and its ^{1}H NMR spectrum in C_6D_6 solution features two sets of peaks of comparable intensity, one of which is broadened and closely resembles that of [**Mo**N$_2$]$^-$ in the spectrum of [Bu$_4$N][**Mo**N$_2$]. (The broadening results from slow exchange with **Mo**N$_2$ impurity; vide supra.) According to IR spectra (Figure 4B), [Mg(DME)$_3$]$_{0.5}$[**Mo**N$_2$] exists as a mixture of [**Mo**N$_2$]$^-$ (1854 cm^{-1}) and [**Mo**N=NMg(DME)$_n$]$^+$ (1770, 1741 cm^{-1}) in benzene. The minor band at 1869 cm^{-1} can be assigned to a "zwitterionic" [**Mo**N$_2$]{Mg(DME)$_n$}$^+$ structure with {Mg(DME)$_n$}$^{2+}$ bound at the equatorial nitrogen(s), similar to the situation discussed above

Table 1. Crystal Data and Structure Refinement for $\{Mg(DME)_3\}_{0.5}[\mathbf{Mo}(N_2)]$, $\mathbf{Mo}(N_2)MgBr(THF)_3$, and $\mathbf{Mo}(N_2)$[a]

paramg	$\{Mg(DME)_3\}_{0.5}[\mathbf{Mo}(N_2)]$	$\mathbf{Mo}(N_2)MgBr(THF)_3$	$\mathbf{Mo}(N_2)$
empirical formula	$C_{144}H_{235}Mg_{0.50}MoN_6O_{15.50}$	$C_{126}H_{183}BrMgMoN_6O_3$	$C_{114}H_{159}MoN_6$
fw	2406.48	2029.95	1709.41
temp (K)	100(2)	183(2)	183(2)
cryst system	monoclinic	monoclinic	monoclinic
space group	*C*2/*c*	*Pn*	*C*2/*c*
unit cell dimens (Å, deg)	$a = 43.611(4)$	$a = 29.131(7)$	$a = 33.485(6)$
	$b = 20.8182(15)$	$b = 17.124(4)$	$b = 20.426(4)$
	$c = 39.304(3)$	$c = 30.065(8)$	$c = 39.081(7)$
	$\alpha = 90$	$\alpha = 90$	$\alpha = 90$
	$\beta = 113.707(3)$	$\beta = 108.920(5)$	$\beta = 99.377(4)$
	$\gamma = 90$	$\gamma = 90$	$\gamma = 90$
V (Å^3)	32673(5)	14187(6)	26372(8)
Z	8	4	8
D (calcd; Mg/m^3)	0.978	0.950	0.861
abs coeff (mm^{-1})	0.135	0.421	0.137
F(000)	10 504	4376	7416
cryst size (mm^3)	0.3 × 0.2 × 0.2	0.08 × 0.14 × 0.35	0.26 × 0.11 × 0.10
θ range (deg)	1.02−26.50	2.07−23.28	1.99−20.00
index ranges	$-54 \le h \le 49$	$-30 \le h \le 32$	$-32 \le h \le 31$
	$0 \le k \le 26$	$-19 \le k \le 18$	$-19 \le k \le 18$
	$0 \le l \le 49$	$-33 \le l \le 21$	$-27 \le l \le 37$
reflcns collcd	33 807	56 374	37 694
indpdt reflcns	33 807 [R(int) = 0.0714]	20 376 [R(int) = 0.1690]	12 263 [R(int) = 0.1385]
completeness to θ max (%)	99.8	99.7	99.5
data/restraints/params	33 807/115/1546	20 376/0/1244	12 263/0/1127
goodness-of-fit on F^2	1.109	1.047	1.051
final R indices [$I > 2\sigma(I)$]	R1 = 0.1022, wR2 = 0.2862	R1 = 0.1196, wR2 = 0.2785	R1 = 0.0723, wR2 = 0.1745
R indices (all data)	R1 = 0.1442, wR2 = 0.3168	R1 = 0.2022, wR2 = 0.3279	R1 = 0.1028, wR2 = 0.1900
largest diff peak and hole (e Å^{-3})	1.483 and −0.684	1.074 and −1.088	0.780 and −0.407

[a] In all cases Mo Kα radiation (0.710 73 Å) was employed and the refinement method was full-matrix least-squares on F^2, except for $\{Mg(DME)_3\}_{0.5}[\mathbf{Mo}N_2]$ (block).

for **Mo**N═NMgCl(THF)$_3$. Since only two sets of ^{1}H NMR peaks are seen in C_6D_6, and exchange between the species responsible for them (i.e., $[\mathbf{Mo}N_2]^-$ and $[\mathbf{Mo}N{=}NMg(DME)_n]^+$) is slow on the NMR time scale, it is possible that $\{Mg(DME)_n\}^{2+}$ readily migrates between N_β and equatorial amide nitrogen(s) of the same $[MoN_2]^-$ ion and exchange-averages species with IR bands at 1869 and 1770, 1741 cm^{-1} on the NMR time scale. However, we stop short of proposing this fluxionality in the absence of VT NMR data. Last, the IR spectrum of $[Mg(DME)_3]_{0.5}[MoN_2]$ in THF after equilibration (∼10 min; Figure 4C) shows that $\{MgTHF_n\}^{2+}$ is capable of binding to N_β of $[MoN_2]^-$, giving rise to the ν_{NN} band at 1808 cm^{-1}. Large, green−black crystals of $\{Mg(DME)_3\}_{0.5}[MoN_2]$ can be isolated from the reaction of **Mo**Cl with Mg in DME, an X−ray structure of which is reported below.

X-ray Structures of Anionic Diazenido Complexes and the Dinitrogen Complex. The compound $\{Mg(DME)_3\}_{0.5}[\mathbf{Mo}N_2]$ was prepared by Mg reduction of **Mo**Cl in DME, and the green-black crystals obtained after crystallization from DME/pentane were subjected to an X-ray crystallographic study using a Bruker CCD detector and Mo Kα radiation (see Tables 1 and 3 and Figure 5). The IR spectrum of the batch of crystals chosen for the X-ray study showed a band at 1852 cm^{-1} ($[\mathbf{Mo}N_2]^-$) and no low-frequency **Mo**N═NMg bands in Nujol. The structure was solved and refined to an R1 value of 10%. The $[\mathbf{Mo}N_2]^-$ anion clearly has nothing bound to N_β. The $[Mg(DME)_3]^{2+}$ cation was found to be disordered between two sites and to exhibit an extra difference density peak within the DME cage, possibly resulting from a hydroxide group or a water molecule. The N−N bond length of the N_2 ligand (1.150(5) Å) in $[\mathbf{Mo}N_2]^-$

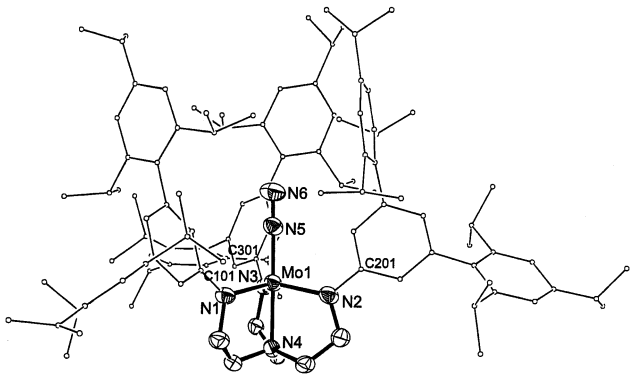

Figure 5. ORTEP diagram (50% ellipsoid probability level) of $[Mg(DME)_3]_{0.5}[\mathbf{Mo}(N_2)]$ (anion only). Hydrogen atoms are omitted for clarity. All non-hydrogen atoms were refined anisotropically.

(Table 3) is slightly shorter yet statistically indistinguishable from that in the related complexes [*t*-Bu$C_6H_4N_3N$]MoN═NNa(15-crown-5) (1.161(5) Å),[13c] $\{[Ph_2C_6H_3N_3N]MoN_2\}_2$-Mg(DME)$_2$ (1.166(12) and 1.173(12) Å),[13c] and **Mo**N═NMgBr(THF)$_3$ (1.156(8) Å; see below), all of which contain Lewis acids coordinated to N_β. These rather small differences in N−N distances with and without Lewis acid coordination to N_β suggest that the $N_\beta\cdots M'$ interaction in [N$_3$N]MoN═NM′ compounds is quite weak, consistent with only a 43 cm^{-1} ν_{N-N} frequency shift observed upon coordination of $MgCl(THF)_3^+$ to $[\mathbf{Mo}N_2]^-$. The mean-square planes of the Trip rings deviate from being strictly orthogonal to the phenyl rings to which they are bound by 5−10°, which is true of all complexes explored here with the exception of **Mo**N═NMgBr(THF)$_3$ (vide infra). The N(5)−Mo−N−C_{ipso} dihedral angles are relatively small (2.5−6.0°), while the Mo−N−

Table 2. Crystal Data and Structure Refinement for **Mo**≡N and {**Mo**(NH$_3$)}{BAr′$_4$}[a]

param	**Mo**≡N	{**Mo**(NH$_3$)}BAr′$_4$}
empirical formula	$C_{114}H_{158}MoN_5$	$C_{146}H_{174}BF_{24}MoN_5$
fw	1694.39	2561.65
temp (K)	188(2)	183(2)
cryst system	Monoclinic	triclinic
space group	$P2_1/n$	$P\bar{1}$
unit cell dimens (Å, deg)	$a = 18.050(3)$ $b = 39.322(6)$ $c = 19.330(3)$ $\alpha = 90$ $\beta = 116.507(3)$ $\gamma = 90$	$a = 15.608(3)$ $b = 20.491(3)$ $c = 26.085(4)$ $\alpha = 84.788(4)$ $\beta = 84.351(4)$ $\gamma = 82.914(4)$
V (Å^3)	12 278(3)	8213(2)
Z	4	2
D (calcd; Mg/m^3)	0.917	1.036
abs coeff (mm^{-1})	0.147	0.149
F(000)	3676	2696
cryst size (mm^3)	0.23 × 0.14 × 0.10	0.10 × 0.05 × 0.05
θ range (deg)	1.63−20.00	1.23−20.00
index ranges	$-17 \le h \le 16$ $-37 \le k \le 23$ $-18 \le l \le 17$	$-15 \le h \le 12$ $-19 \le k \le 19$ $-25 \le l \le 25$
reflcns collcd	39 261	29 517
indpdt reflcns	11 458 [R(int) = 0.1089]	15 296 [R(int) = 0.1064]
completeness to $\theta = 20.00°$ (%)	99.9	99.9
data/restraints/params	11 458/0/1082	15 296/0/1601
goodness-of-fit on F^2	1.078	1.111
final R indices [$I > 2\sigma(I)$]	R1 = 0.0805, wR2 = 0.1850	R1 = 0.1278, wR2 = 0.3028
R indices (all data)	R1 = 0.1046, wR2 = 0.1953	R1 = 0.1566, wR2 = 0.3235
largest diff peak and hole (e Å^{-3})	0.487 and −0.796	1.561 and −1.018

[a] In all cases Mo Kα radiation (0.710 73 Å) was employed and the refinement method was full-matrix least-squares on F^2.

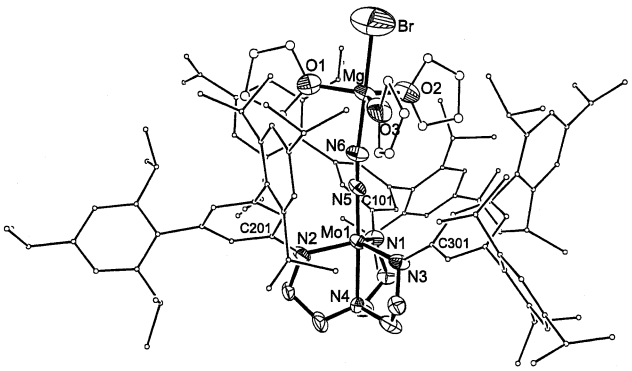

Figure 6. An ORTEP diagram (50% ellipsoid probability level) of **Mo**N═NMgBr(THF)$_3$. Hydrogen atoms are omitted for clarity. All non-hydrogen atoms were refined anisotropically.

$C_{ipso}-C_o$ dihedral angles vary from 32.3 to 33.9°. The inner aryl (Ar(i)) rings are rotated by an average of 25.5° out of the plane of amido nitrogens.

The X-ray study of **Mo**N$_2$MgBr(THF)$_3$ (Tables 1 and 3; Figure 6) reveals a trigonal bipyramidal Mg bound to the β nitrogen. The 3 equiv of THF occupy approximate equatorial positions around the magnesium. The relatively large MgBr(THF)$_3$ unit forces the "pocket" to open considerably from that in the structure of {Mg(DME)$_3$}$_{0.5}$[**Mo**N$_2$], as evidenced by (i) larger N(5)−Mo−N−C_{ipso} dihedral angles (∼23° (average) vs ∼5° (average) in the free anion) and (ii) smaller dihedral angles between the mean planes of the Ar(i) (inside) and Ar(o) (TRIP) ring facing the apical pocket (58.7−70.9°) compared to the TRIP ring pointing away from the apical pocket (87.7−88.3°). The N(5)−N(6) bond length (1.156(8) Å) is virtually the same as in the free anion (1.150(5) Å), although the Mo−N(5) bond length is marginally shorter (by 0.05 Å). Other differences between the structure of **Mo**N$_2$MgBr(THF)$_3$ and the free anion are relatively insignificant. The steric hindrance present in the structure of **Mo**N$_2$MgBr(THF)$_3$ at least partly promotes dissociation of THF bound to Mg and dissociation of [MgClL_n]$^+$ (L = THF, DME).

The X-ray structure of **Mo**(N$_2$) (Tables 1 and 3; Figure 7) closely resembles that of [**Mo**N$_2$]$^-$, except the Mo−N(4) bond length is slightly shorter and the Mo−N(5) bond length slightly longer, consistent with one electron having been removed from the Mo−N(4)−N(5) system. Consistent with this fact also, the Mo−N_{amido} bond lengths are slightly shorter and the Mo−N_{amido}−C_{ipso} bond angles are slightly smaller. The N(5)−Mo−N−C_{ipso} dihedral angles are again of the same order as in the free anion, but the dihedral angles between the amido nitrogen plane and Ar(i) (58.4° average) are the largest of any in the three structures. As evident from the shape of thermal ellipsoids in Figure 7, the dinitrogen ligand in **Mo**N$_2$ suffers from excessive thermal motion, the extent of which is notably greater than that in the case of anionic [**Mo**N$_2$]$^-$ derivatives, consistent with the weaker Mo−N$_2$ π-bonding in the neutral species. As a result, the N−N distance of 1.061(7) Å in Mo−N$_2$ is artificially "short" compared to that in free N$_2$ (1.098 Å).[24]

Synthesis of [HIPTN$_3$N]MoN═NH and Its Conversion to [HIPTN$_3$N]MoH and {[HIPTN$_3$N]Mo═NNH$_2$}$^+$. It was noticed that a diamagnetic impurity formed readily upon reaction of [**Mo**N$_2$]$^-$ with traces of moisture. We proposed that this impurity was the parent diazenido species, **Mo**N═NH. Initial attempts to prepare it on a large scale revealed that attempted protonation of [**Mo**N$_2$]$^-$ derivatives also led to 1e$^-$ oxidation of [**Mo**N$_2$]$^-$ to give **Mo**N$_2$. However, we found that **Mo**N═NH could be prepared by treating [**Mo**N$_2$]$^-$, produced upon reduction of **Mo**Cl by magnesium in THF, with [Et$_3$NH][OTf] (eq 7). An ^{15}N-labeled sample was prepared in 72% yield by adding solid [Bu$_4$N][**Mo**^{15}N$_2$] to a cold ether solution of [Et$_3$NH][BAr′$_4$] (Ar′ = 3,5-(CF$_3$)$_2$C$_6$H$_3$) (eq 8).

$$[HIPTN_3N]MoCl \xrightarrow[2.\ [Et_3NH][OTf]]{1.\ 10Mg,\ 0.5BrCH_2CH_2Br,\ THF,\ 2\ h} [HIPTN_3N]MoN{=}NH \quad (7)$$

$$[Et_3NH][BAr'_4] \xrightarrow[2.\ solid\ [Bu_4N]\mathbf{Mo}N_2]{1.\ Et_2O,\ -25\ °C} [HIPTN_3N]MoN{=}NH \quad (8)$$

The proton NMR spectrum of **Mo**N═NH (in C$_6$D$_6$ at 20 °C) reveals the diazenido proton resonance at 8.57 ppm. In **Mo**^{15}N═^{15}NH this resonance is a doublet of doublets with $^1J(^{15}N_\beta-H)$ = 53.6 Hz and $^2J(^{15}N_\alpha-H)$ = 7.9 Hz. The ^{15}N

(24) Although this phenomenon could be attributed to a Jahn−Teller distortion of the **Mo**N$_2$ structure involving a slight bending of the N$_2$ ligand, we note that the structure of [N(CH$_2$CH$_2$NH)$_3$]Mo(N$_2$) was computed to deviate marginally from C_{3v} symmetry in its ground ^{2}A state.[21]

Table 3. Selected Bond Lengths (Å) and Angles (deg) in $\{Mg(DME)_3\}_{0.5}$[**Mo**(N_2)], **Mo**(N_2)MgBr(THF)$_3$, and **Mo**(N_2)

	$\{Mg(DME)_3\}_{0.5}$[**Mo**(N_2)]	**Mo**(N_2)MgBr(THF)$_3$	**Mo**(N_2)
Mo−N(1)	2.045(3)	2.035(6)	1.983(5)
Mo−N(2)	2.028(4)	2.029(6)	1.976(4)
Mo−N(3)	2.032(3)	2.026(6)	1.974(4)
Mo−N(4)	2.210(3)	2.241(6)	2.188(4)
Mo−N(5)	1.913(4)	1.863(7)	1.963(5)
N(5)−N(6)	1.150(5)	1.156(8)	1.061(7)
Mg−N(6)		2.073(8)	
N(5)−Mo−N(1)	98.49(14)	102.4(3)	99.4(2)
N(5)−Mo−N(2)	99.65(15)	98.6(3)	98.9(2)
N(5)−Mo−N(3)	99.70(14)	98.6(3)	99.1(2)
N(5)−Mo−N(4)	179.19(15)	177.4(3)	179.8(2)
N(4)−Mo−N(1)	80.70(13)	80.5(2)	80.45(17)
N(4)−Mo−N(2)	80.86(13)	79.9(3)	81.28(16)
N(4)−Mo−N(3)	80.60(12)	80.2(2)	80.90(17)
N(3)−Mo−N(1)	116.84(13)	116.0(3)	118.25(18)
N(3)−Mo−N(2)	116.75(14)	119.1(3)	116.36(18)
N(2)−Mo−N(1)	118.77(15)	116.2(3)	117.99(18)
Mo−N(1)−C(101)	131.0(3)	134.1(5)	127.4(3)
Mo−N(2)−C(201)	130.6(3)	134.1(5)	129.4(3)
Mo−N(3)−C(301)	131.0(3)	134.4(5)	128.5(3)
Mo−N(5)−N(6)	179.2(4)	178.7(7)	179.2(7)
N(5)−Mo−N(1)−C(101)	2.5(4)	21.5(8)	5.4(5)
N(5)−Mo−N(2)−C(201)	7.6(4)	25.2(8)	8.9(5)
N(5)−Mo−N(3)−C(301)	6.0(3)	22.7(8)	6.2(5)
Mo−N(1)−C(101)−C_{ortho}	32.3	28.8	67.3
Mo−N(2)−C(201)−C_{ortho}	33.9	27.1	69.2
Mo−N(3)−C(301)−C_{ortho}	32.4	31.4	67.3
Ar(o)/Ar(i)[a]	81.9 (79.5−85.1)	88.7 (87.7−89.5) 66.3 (58.7−70.9)	86.4 (77.3−89.4)
Ar(i)/N(plane)[b]	25.5 (24.3−26.1)	33.6 (31.0−35.0)	58.4 (58.2−58.7)

[a] Average angle (range) between the mean square planes of the phenyl ring attached to the amido nitrogen (Ar(i)) and the Trip rings (Ar(o)). [b] Average angle (range) between the mean-square planes of the amide nitrogen and that of the phenyl ring (Ar(i)) bound to it.

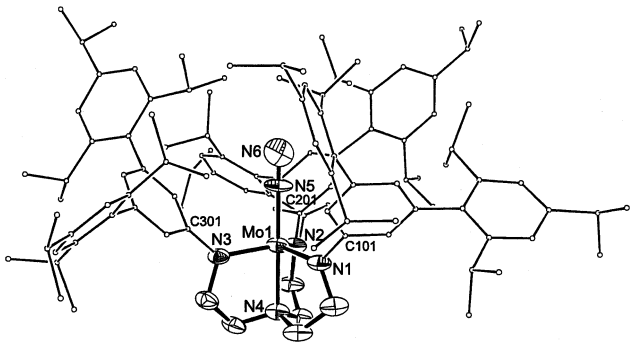

Figure 7. ORTEP diagram (50% ellipsoid probability level) of **Mo**(N_2). Hydrogen atoms are omitted for clarity. All non-hydrogen atoms were refined anisotropically.

NMR spectrum of **Mo**^{15}N═^{15}NH reveals the resonance for N_α at 409.0 ppm ($J(^{15}N_\alpha-^{15}N_\beta)$ = 15.7 Hz) and the resonance for N_β at 232.6 ppm. Comparison of IR data for the ^{15}N-labeled compound (in italics) with those for the unlabeled compound allowed us to assign the essential stretches: ν_{N-N} 1587 (*1523*) and ν_{N-H} 3135 (*3129*) cm^{-1} in C_6D_6. As is the case with most other **Mo**N_xH_y complexes described here, the ν_{N-H} band of **Mo**N═NH is weak and is found as a shoulder on the strong set of ν_{C-H} absorptions; it was assigned tentatively on the basis of the observed 6 cm^{-1} shift on $^{15}N/^{14}N$ substitution (7 cm^{-1} calculated from the isotope ratio). The only other band in the IR spectrum of **Mo**N═NH that shifts upon $^{15}N_2/^{14}N_2$ substitution is that at 1137 cm^{-1} (*1125* cm^{-1}, both in C_6D_6). On the basis of computational studies of related model systems,[25] this band is assigned to an N−N−H bending vibration. The ^{15}N NMR chemical shifts and $J(^{15}N-H)$ coupling constants of **Mo**^{15}N═^{15}NH and other ^{15}N-labeled complexes described here are similar to those of closely related compounds[25] and fall well within the ranges established for other compounds of this general type.[26,27]

The diazenide derivative **Mo**N═NH prepared as shown in eq 7 decomposes at 61 °C in C_6D_6 in a first-order fashion (Figure 8A, $k_1 = 2.68(5) \times 10^{-5}$ s^{-1}, half-life ∼ 7 h) to yield the paramagnetic hydride derivative **Mo**H (vide infra) as the major product, along with a small amount of unidentified impurities (eq 9). The rate of this decomposition in aliphatic solvents is similar to its rate in C_6D_6. Slow decomposition of **Mo**N═NH into **Mo**H in solution at ambient temperature has so far thwarted all attempts to obtain X-ray-quality crystals of **Mo**N═NH. (While relatively pure **Mo**N═NH is difficult to crystallize from pentane, **Mo**N═NH and **Mo**H, a much less soluble compound, *cocrystallize* readily from pentane.) Traces of **Mo**H are also found upon heating **Mo**N═NH in the solid state under vacuum at 60 °C for several hours. However, a sample prepared according to the reaction shown in eq 7 remained unchanged by ^{1}H NMR after being stored at −25 °C for 17 months.

$$[HIPTN_3N]MoN{=}NH \xrightarrow{\text{heat in } C_6D_6} [HIPTN_3N]MoH \quad (9)$$

In contrast, samples of **Mo**N═NH prepared as shown in eq 8 (utilizing 1.05 equiv of $[Et_3NH][BAr'_4]$) decompose at

(25) Dmitry V. Khoroshun, personal communication.
(26) Mason, J. *Chem. Rev.* **1981**, *81*, 205.
(27) Mason, J. In *Multinuclear NMR*; Mason, J., Ed.; Plenum: New York, 1987.

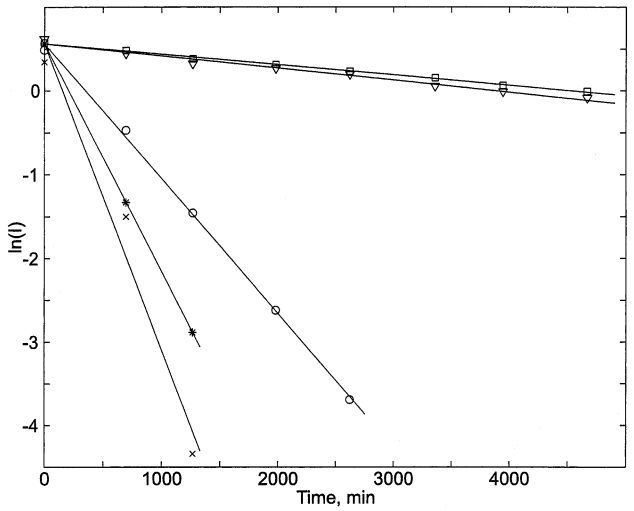

Figure 8. Decay of **Mo**N═NH in C_6D_6 at 61(±2) °C monitored by ^{1}H NMR ($[Mo]_{tot} \sim 15$ mM). **Mo**N═NH was prepared according to the method shown in eq 7 (A, circles), eq 8 with 1.05 equiv of acid (B, squares), and eq 8 with 0.9 equiv of acid (C, triangles). Decay of **Mo**N═NH prepared according to eq 8 with 1.05 equiv of acid is also shown in the presence of ~0.8 mol % of $[Et_3NH][OTf]$ (D, *) and $[Et_3NH][BAr'_4]$ (E, ×), each used as a 35 mM solution in PhF. All runs were performed side-by-side.

61 °C in C_6D_6 over 10 times more slowly (Figure 8B, $k_1 = 2.07(5) \times 10^{-6}$ s^{-1}) than samples prepared as shown in eq 7. Addition of ~0.8 mol % of either $[Et_3NH][OTf]$ (Figure 8D) or $[Et_3NH][BAr'_4]$ (Figure 8E) to this sample leads to an accelerated first-order decomposition ($k_1 = 4.5(1) \times 10^{-5}$ s^{-1} and $k_1 = 6.1(8) \times 10^{-5}$ s^{-1}, respectively). Therefore, we suspect that a small amount of a proton source is present in **Mo**N═NH when it is prepared by eq 7 and that impurity accelerates decomposition of **Mo**N═NH. Attempts to exclude acidic impurities in **Mo**N═NH completely, e.g., by reacting $[Bu_4N][\mathbf{Mo}N_2]$ with only 0.9 equiv of $[Et_3NH][BAr'_4]$, afforded a solid (41% yield, triply recrystallized) that decomposed at 61 °C with $k_1 = 2.4(1) \times 10^{-6}$ s^{-1} (Figure 8C), which is statistically indistinguishable from that of the material prepared with 1.05 equiv of $[Et_3NH][BAr'_4]$ (Figure 8B). Therefore, we consider $k_1 = 2.2 \times 10^{-6}$ s^{-1} (the average obtained for the highest purity materials) to be the upper limit for the rate constant for any uncatalyzed "β-hydrogen elimination" from **Mo**N═NH. It is also notable that while all runs presented in Figure 8 led to formation of predominantly **Mo**H, with only a small amount of unidentified products being formed, catalysis of the decomposition of **Mo**N═NH by $[Et_3NH][BAr'_4]$ (run E) also resulted in formation of ~20% of $\mathbf{Mo}N_2$, a trace impurity that inevitably is present in all other samples, but remains constant throughout runs A−D. We conclude that traces (<1 mol %) of acidic impurities (e.g. $[Et_3NH][OTf]$ or $H_3[HIPTN_3N]$·HOTf) catalyze the decomposition of **Mo**N═NH prepared by the method shown in eq 7, even though both ^{1}H and ^{19}F NMR spectra of this material are devoid of signals assignable to such species. Therefore, the method shown in eq 8 is the preferred method for preparing **Mo**N═NH (67% yield). Exactly how "β-hydrogen elimination" from **Mo**N═NH proceeds or how the decomposition of **Mo**N═NH is accelerated in the presence of traces of acid remains highly speculative.

The paramagnetic hydride complex **Mo**H was isolated as a bright brick-red solid in 62% yield by heating a solution of **Mo**N═NH prepared by the method shown in eq 7 for 4 days at 60 °C in heptane. Although **Mo**Cl so far has remained inert to a variety of hydride sources, preliminary results suggest that the reaction between $[\mathbf{Mo}(NH_3)][BAr'_4]$ (vide infra) and $LiBHEt_3$ (1 M in THF) in C_6D_6 yields **Mo**H in >90% yield according to ^{1}H NMR spectra. The ^{1}H NMR spectrum of **Mo**H in C_6D_6 features the paramagnetically broadened resonances for the isopropyl group, *para*-aromatic, and *meta*-aromatic protons, while the expected high-field backbone signals and *ortho*-aromatic resonances are not observed at 22 °C. These findings contrast with the spectroscopic data obtained for the related $[TMSN_3N]MoH$ species,[28] where backbone resonances were observable in the ^{1}H NMR spectrum. The IR spectrum of **Mo**H features a relatively strong ν_{Mo-H} absorption at 1748 cm^{-1} (in C_6D_6, 1751 cm^{-1} in Nujol), shifted by 70 cm^{-1} to higher energies from that observed in the $[TMSN_3N]MoH$. When a C_6D_6 solution of **Mo**H was placed under an atmosphere of D_2, HD was observed by ^{1}H NMR after 50 min and an IR spectrum of the solution showed also a ν_{Mo-D} band at 1252 cm^{-1} (a shift of 496 cm^{-1}; cf. 505 cm^{-1} expected from the isotope ratio). Additional studies involving **Mo**H will be reported in due course.

Protonation of **Mo**N═NH with $[H(OEt_2)_2][BAr'_4]$ in C_6D_6 ($Ar' = 3,5\text{-}(CF_3)_2C_6H_3$) afforded $[Mo{=}NNH_2][BAr'_4]$ nearly quantitatively in 2 h at 22 °C (by ^{1}H NMR). The salt was isolated in 68% yield from the analogous reaction in ether (1.5 h) and fully characterized. The hydrazido protons appear as a singlet at 6.66 ppm in the ^{1}H NMR spectrum in C_6D_6. Like other $BAr'_4{}^-$ salts described here, crude $[\mathbf{Mo}{=}NNH_2][BAr'_4]$ is highly soluble, even in pentane. However, as is the case with all other $BAr'_4{}^-$ derivatives described here, crystallization from crude mixtures can be accomplished by seeding with a small amount of crystalline sample, originally obtained by prolonged storage of a pentane solution at −25 °C in a vial closed with a Teflon-lined cap, which appears to initiate crystallization. The crystallized material is soluble in pentane and can be recrystallized readily without seeding. The $^{15}N_2$ derivative was generated in situ in an NMR tube in C_6D_6. The hydrazido proton resonance is split into a doublet of doublets ($^1J(^{15}N_\beta{-}H) = 90.5$ Hz, $^2J(^{15}N_\alpha{-}H) = 1.4$ Hz), while the ^{15}N NMR spectrum features a doublet at 357.5 ppm for $^{15}N_\alpha{=}^{15}N_\beta H_2$ and a triplet of doublets at 140.0 ppm for $^{15}N_\alpha{=}^{15}N_\beta H_2$ ($J(^{15}N_\alpha{-}^{15}N_\beta) = 11$ Hz). The IR spectrum of $[\mathbf{Mo}{=}NNH_2][BAr'_4]$ in C_6D_6 features two weak bands at 3379 and 3274 cm^{-1} that shift to 3370 and 3270 cm^{-1}, respectively, in the spectrum of $[\mathbf{Mo}{=}{}^{15}N^{15}NH_2][BAr'_4]$. Therefore, these absorptions were assigned to the asymmetric and symmetric ν_{N-H} stretches, respectively.

Synthesis of [HIPTN$_3$N]Mo≡N and {[HIPTN$_3$N]Mo≡NH}$^+$. Heating a C_6D_6 solution of **Mo**Cl with 2.0 equiv of Me_3SiN_3 at 90 °C resulted in a slow formation of a single diamagnetic product, **Mo**≡N, along with Me_3SiCl; the

(28) Schrock, R. R.; Seidel, S. W.; Mösch-Zanetti, N. C.; Shih, K.-Y.; O'Donoghue, M. B.; Davis, W. M.; Reiff, W. M. *J. Am. Chem. Soc.* **1997**, *119*, 11876.

conversion was quantitative after ~3 days. Sodium azide also reacted with **Mo**Cl to afford a moderate yield of **Mo**≡N in THF at room temperature after 2 days, although a small amount of the free ligand was also formed in this case. Using Me_3SiN_3, **Mo**≡N could be isolated in 77% yield as a bright yellow crystalline solid. The solubility of **Mo**≡N in pentane was limited, i.e., comparable to that of **Mo**Cl. The reaction between 50% terminally ^{15}N-labeled sodium azide and **Mo**Cl gave 50% ^{15}N-labeled nitride, **Mo**≡$^{15/14}$N. The nitride nitrogen appears as a singlet at 898 ppm in the ^{15}N NMR spectrum, and comparison of the IR spectra of **Mo**≡$^{15/14}$N and **Mo**≡^{14}N allowed us to assign ν_{MoN} = 1013 cm^{-1} in **Mo**≡^{14}N (*986* in **Mo**≡^{15}N).

Protonation of **Mo**≡N with [H(OEt$_2$)$_2$][BAr′$_4$] in C_6D_6 afforded [**Mo**═NH][BAr′$_4$]. At 20 min after the reagents were mixed in an NMR tube in C_6D_6, an ^{1}H NMR spectrum showed that **Mo**≡N had been converted largely into [**Mo**═NH]$^+$; however, other diamagnetic products were also present in significant, but variable, amounts. We suspect that a proton is also added to the ligand's amido nitrogen or to the inverted amine donor; multiple protonations of the ligand in the same complex also cannot be ruled out. Nevertheless, the system evolves into [**Mo**═NH]$^+$ nearly quantitatively after 24 h. The [**Mo**═NH][BAr′$_4$] salt was isolated in 93% yield from the analogous reaction in ether (1 h) and fully characterized. The imido proton is found as a singlet at 6.59 ppm in the ^{1}H NMR spectrum in C_6D_6. The compound was crystallized as described above for [**Mo**═NNH$_2$][BAr′$_4$] and found to exhibit good solubility in pentane.

The 50% ^{15}N-labeled derivative, [**Mo**═$^{15/14}$NH]$^+$, was prepared analogously from **Mo**≡$^{15/14}$N. The imido proton resonance at 6.59 ppm is flanked by ^{15}N satellites $^1J(^{15}N-H)$ = 73.7 Hz, and a doublet is observed at 427.7 ppm in the ^{15}N NMR spectrum. Comparison of the IR spectra of [**Mo**═NH]$^+$ and [**Mo**═$^{15/14}$N]$^+$ in C_6D_6 allowed us to assign the moderate bands at 3341 and 3334 cm^{-1} to $\nu^{14}{}_{N-H}$ and $\nu^{15}{}_{N-H}$, respectively; no other bands that shifted upon ^{15}N/^{14}N substitution were observed.

Synthesis of {[HIPTN$_3$N]Mo(NH$_3$)}$^+$. No reaction was observed upon treatment of **Mo**Cl with NaBAr′$_4$ in CD_2Cl_2, while addition of NH_3 alone to **Mo**Cl only causes formation of a small amount of free ligand. However, the combination of the two reagents yielded the cationic ammonia adduct [**Mo**(NH$_3$)][BAr′$_4$]. Employing $NaBPh_4$ and ammonia led to [**Mo**(NH$_3$)][BPh$_4$] in high yield. While use of thallium salts, TlOTf and $TlPF_6$, readily afforded the corresponding OTf$^-$ and PF_6^- derivatives, these salts displayed poor thermal stability and were not isolated. All reactions are typically accompanied by formation of a small amount of the free ligand, even though NH_3 is vacuum-transferred from a bronze-colored solution of Na and all other precautions are taken to exclude moisture and air. The BAr′$_4^-$ and BPh_4^- salts have been isolated in 80% and 71% respective yields and fully characterized. The BAr′$_4^-$ salt is highly soluble in pentane when impure but can be crystallized readily if relatively pure, as described above for [**Mo**═NNH$_2$][BAr′$_4$]. The BPh_4^- salt can be crystallized readily from pentane. [**Mo**(NH$_3$)][BPh$_4$] is converted into [**Mo**(NH$_3$)][BAr′$_4$] upon treatment with NaBAr′$_4$ in CD_2Cl_2. Proton NMR spectra of both compounds show the backbone methylene proton resonances at −21 and −103 ppm in C_6D_6 and −18 and −106 ppm in CD_2Cl_2. The *o*-CH signal is strongly broadened and obscured in the aromatic region at ~6 ppm, while the *p*-CH resonance is found at −2.6 ppm (in C_6D_6) or −4.7 ppm (in CD_2Cl_2) with BAr′$_4^-$ as the anion and at −0.6 ppm (in C_6D_6) or −4.1 ppm (in CD_2Cl_2) with BPh_4^- as the anion. Since all reactions of **Mo**Cl with ammonia and the Cl$^-$-abstracting salts are complete at room temperature in CD_2Cl_2 within 30 min, it appears likely that ammonia displaces chloride from **Mo**Cl in a preequilibrium, which is driven to completion by reaction with the sodium salts of weakly coordinating anions to give NaCl.

Table 4. Selected Bond Lengths (Å) and Angles (deg) in **Mo**≡N and {**Mo**(NH$_3$)}{BAr′$_4$} (Cation Only)

	Mo≡N	{**Mo**(NH$_3$)}{BAr′$_4$}
Mo−N(1)	2.001(5)	1.979(9)
Mo−N(2)	2.007(5)	1.944(8)
Mo−N(3)	2.001(5)	1.920(10)
Mo−N(4)	2.395(5)	2.147(9)
Mo−N(5)	1.652(5)	2.236(10)
N(5)−Mo−N(1)	102.6(2)	99.2(4)
N(5)−Mo−N(2)	101.6(2)	98.2(4)
N(5)−Mo−N(3)	101.8(2)	99.0(4)
N(5)−Mo−N(4)	179.1(2)	178.5(4)
N(4)−Mo−N(1)	78.23(18)	82.2(4)
N(4)−Mo−N(2)	78.42(19)	80.7(4)
N(4)−Mo−N(3)	77.4(2)	80.8(4)
N(3)−Mo−N(1)	115.8(2)	117.2(4)
N(3)−Mo−N(2)	117.1(2)	119.6(4)
N(2)−Mo−N(1)	114.5(2)	116.4(4)
Mo−N(1)−C(101)	128.8(4)	128.2(8)
Mo−N(2)−C(201)	128.8(4)	126.7(7)
Mo−N(3)−C(301)	128.2(4)	129.1(7)
N(5)−Mo−N(1)−C(101)	3.5(6)	19.5(10)
N(5)−Mo−N(2)−C(201)	6.3(6)	8.1(10)
N(5)−Mo−N(3)−C(301)	2.6(6)	12.6(10)
Mo−N(1)−C(101)−C$_{ortho}$	34.0	80.8
Mo−N(2)−C(201)−C$_{ortho}$	33.7	74.4
Mo−N(3)−C(301)−C$_{ortho}$	34.0	75.0
Ar(o)/Ar(i)[a]	86.7 (83.2−89.2)	86.3 (80.9−89.9)
Ar(i)/N(plane)[b]	27.5 (27.1−28.2)	67.4 (64.9−69.3)

[a] Average angle (range) between the mean-square planes of the phenyl ring attached to the amido nitrogen (Ar(i)) and the Trip rings (Ar(o)). [b] Average angle (range) between the mean-square planes of the amide nitrogen and that of the phenyl ring (Ar(i)) bound to it.

X-ray Studies of Mo≡N and {[HIPTN$_3$N]Mo(NH$_3$)}-[BAr′$_4$]. Large crystals of **Mo**≡N could be obtained from a pentane solution and were subjected to an X-ray crystallographic study using a Bruker Apex detector and Mo Kα radiation (see Tables 2 and 4; Figure 9). Solution of the structure (R1 = 8%) revealed a typical trigonal-bipyramidal coordination geometry at Mo with a Mo−N(4) bond length 0.15−0.20 Å longer than that in all other structures (Tables 3 and 4), consistent with the strong trans-influence of the nitride. The Mo≡N bond distance of 1.652(5) Å agrees well with the known Mo−N distance of 1.658(5) Å in Mo(N)-[NPh(*t*-Bu)]$_3$.[7] The Mo−N−C$_{ipso}$−C$_{ortho}$ and N(5)−Mo−N−C$_{ipso}$ dihedral bond angles are similar to what they are in [**Mo**N$_2$]$^-$, which places one of the Trip rings pointing more or less "away" from the metal center and one pointing "up".

An X-ray study of {[HIPTN$_3$N]Mo(NH$_3$)}[BAr′$_4$] (Tables 2 and 4; Figures 10 and 11) reveals that the structure of the

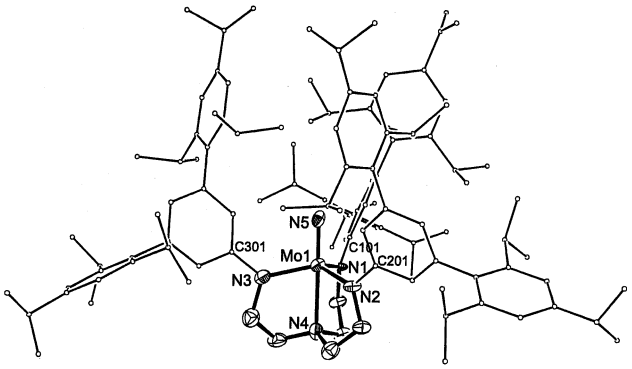

Figure 9. ORTEP diagram (50% ellipsoid probability level) of **Mo**≡N. Hydrogen atoms are omitted for clarity. All non-hydrogen atoms were refined anisotropically.

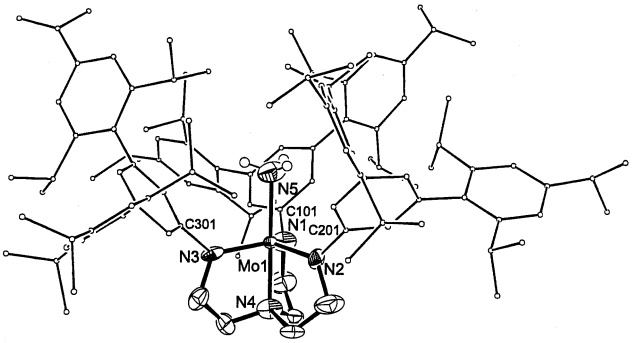

Figure 10. ORTEP diagram (50% ellipsoid probability level) of the [**Mo**(NH$_3$)]$^+$ ion in [**Mo**(NH$_3$)][BAr′$_4$]. Hydrogen atoms (except for NH$_3$) are omitted for clarity. All non-hydrogen atoms were refined anisotropically.

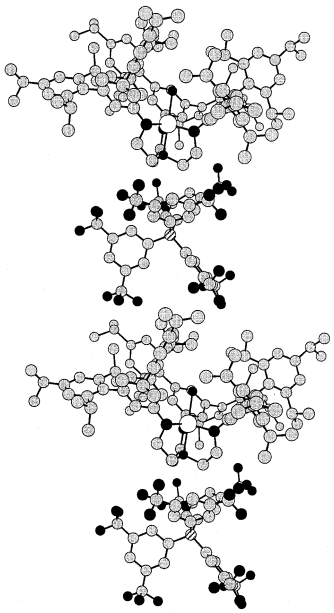

Figure 11. Chem 3D model showing two cation/anion pairs of [**Mo**(NH$_3$)][BAr′$_4$] in a crystal packing fragment. Hydrogen atoms are omitted for clarity.

cation is much like the structure of the dinitrogen complex. The dihedral angles between the amido nitrogen plane and Ar(i) are the largest of any in the five structures presented here. The relatively long Mo−N(5) distance (2.236(10) Å) is in keeping with the two electron donor character of the Mo−NH$_3$ bond. The ammonia protons could not be located. The crystal lattice of {[HIPTN$_3$N]Mo(NH$_3$)}[BAr′$_4$] provides unique structural data on ion pairing between BAr′$_4^-$ and a *larger* cation. In particular, chains of alternating ions with closest approach of the anion to the Mo site can be distinguished (Figure 11), in which the [BAr′$_4$]$^-$ sits more or less "above" one cation, with one of the 3,5-bis-(trifluoromethyl)phenyl rings pointing toward the apical cavity, and "below" another cation, which distantly "docks" onto the faces of two of the 3,5-bistrifluoromethylphenyl rings. However, approach to the metal site from either axial or equatorial directions remains relatively unobstructed and the shortest F···C contact (3.332 Å) in fact involves a backbone methylene carbon.

Comparison of the accumulated structural data for [HIPTN$_3$N]Mo derivatives (Tables 3 and 4) shows that the tetradentate [HIPTN$_3$N] ligand prefers to adopt a conformation at Mo in which the N(5)−Mo−N$_{amide}$−C$_{ipso}$ dihedral angle is around 10° or less and in which the two Ar(o)/Ar(i) angles are both close to 90°. However, rotation of the terphenyl groups around N$_{amide}$−C$_{ipso}$ bonds is relatively facile; e.g., the average Ar(i)/N(plane) angles in **Mo**(N$_2$) and **Mo**≡N, which are both unperturbed by interionic packing forces that are potentially influential in the structures of the ionic derivatives, are considerably different (58.4 and 27.5°, respectively).

Conclusions

On the basis of the results reported here we conclude that the [HIPTN$_3$N]$^{3-}$ ligand dramatically stabilizes a variety of complexes that contain dinitrogen in various stages of reduction against bimolecular decomposition. X-ray studies show that the [HIPTN$_3$N]$^{3-}$ ligand, while quite sterically demanding, is flexible enough to adapt to a variety of circumstances by altering the angle between the Ar(i) ring and the amido ligand plane. However, no clear pattern of response to the size of the group in the apical pocket has emerged on the basis of the five structures we have in hand so far. Six of the compounds that we have isolated (**Mo**(N$_2$), **Mo**≡N, **Mo**N═NH, [**Mo**═NH]$^+$, [**Mo**(NH$_3$)]$^+$, and [**Mo**═NNH$_2$]$^+$) are among the dozen intermediates that one might expect to be part of a 6 proton/6 electron sequence in which end-on bound dinitrogen is reduced to ammonia.[29,30] Since several individual steps in such a reduction sequence have been demonstrated in a preliminary fashion,[14] we believe that there is a good possibility that dinitrogen actually can be reduced catalytically to ammonia with protons and electrons and a properly designed catalyst under the appropriate conditions. Future studies will be aimed toward these goals with complexes that contain the [HIPTN$_3$N]$^{3-}$ ligand and with analogous species that contain variations of the [HIPTN$_3$N]$^{3-}$ ligand such as the hexa-*tert*-butylterphenyl-substituted ligand.

Experimental Section

General Methods. All manipulations of air- and moisture-sensitive compounds were carried out by standard Schlenk and glovebox techniques under an atmosphere of dinitrogen using flame-

(29) Chatt, J.; Dilworth, J. R.; Richards, R. L. *Chem. Rev.* **1978**, *78*, 589.
(30) Pickett, C. J. *J. Biol. Inorg. Chem.* **1996**, *1*, 601.

and oven-dried glassware. Ether, pentane, and toluene were purged with nitrogen, passed through activated alumina columns, and degassed (freeze−pump−thaw) three times. THF, DME, 1,4-dioxane, and benzene were distilled from dark purple Na/benzophenone ketyl solutions. CH_2Cl_2 and MeCN were distilled from CaH_2 under N_2. All dried and deoxygenated solvents were stored over molecular sieves in a nitrogen-filled glovebox. The bulk solvents (THF, DME, ether, pentane, heptane, benzene, tetramethylsilane) were vacuum transferred from dark-purple solutions/suspensions of Na/benzophenone ketyl (CH_2Cl_2 from CaH_2), degassed, and stored under N_2 in flame-dried gastight storage flasks, whenever possible. C_6D_6 was vacuum-transferred from dark purple Na/benzophenone ketyl suspension and CD_2Cl_2 from CaH_2. These solvents were degassed and stored in gastight solvent bulbs inside the glovebox. 1,3,5-Triisopropylbenzene, 2,4,6-tribromoaniline (Lancaster), anhydrous $ZnCl_2$, magnesium (−50 mesh, washed with dilute HCl, water, THF, and ether and dried at 100 °C/10^{-4} Torr for 2 days), $(Me_3Si)_2NLi$ (sublimed; Aldrich), $N(CH_2CH_2NH_2)_3$, NaO-*t*-Bu, $Pd_2(dba)_3$, *rac*-BINAP, $MoCl_5$ (Strem), $^{15}N_2$, NaN_3(1-^{15}N), $^{15}NH_3$ (CIL), and Me_3SiN_3 (Acros) were used as received, unless indicated otherwise. Bromo-2,4,6-triisopropylbenzene,[31] iodo-2,4,6-tribromobenzene[32] (prepared in a manner analogous to that used to prepare iodo-2,6-dibromobenzene),[15] $NaBAr'_4$ ($Ar' = C_6H_3$-3,5-$(CF_3)_2$),[33] $[H(OEt_2)_2][BAr'_4]$,[33] and $MoCl_4(THF)_2$[34] were prepared according to the published procedures or slight modifications thereof. $[Et_3NH][BAr'_4]$ was prepared from Et_3NHCl and 1.05 equiv of $NaBAr'_4$ in CH_2Cl_2. All Mo complexes were stored under N_2 at −25 °C in the dark. ^{1}H, ^{19}F, and ^{15}N NMR spectra were referenced to the residual protio solvent peaks (^{1}H) or external PhF (^{19}F, −113.15 ppm relative to $CFCl_3$) or MeCN (^{15}N, +245.5 ppm relative to neat NH_3 at 303 K[35]). IR spectra were recorded on a Nicolet Avatar 360 FT-IR spectrometer in a demountable solution cell (0.2 mm Teflon spacer, KBr windows). Sealed precision path length (0.208(1) mm) cell with amalgamated KBr windows and a metal spacer were used for the strongly reducing $[\mathbf{Mo}N_2]^-$ derivatives. Solid-state IR spectra were recorded as Nujol mulls. Frequencies and integrated absorbance values (*A*) are given in cm^{-1}. Elemental analyses were performed by H. Kolbe Mikroanalytisches Laboratorium, Mülheim an der Ruhr, Germany.

5′-Bromo-2,4,6,2″,4″,6″-hexaisopropyl-[1,1′:3′,1″]terphenyl (HIPTBr). A 5 L three-necked round-bottom flask equipped with a 250 mL addition funnel, an efficient condenser, and a magnetic stirbar was charged with Mg turnings (48.90 g, 2.01 mol, dried under full vacuum at 120 °C for 2 days) and maintained under a dinitrogen atmosphere throughout. A THF (100 mL) solution of 1,2-dibromoethane (5 mL, 60 mmol) was added to activate the Mg. The volume was increased with THF to 500 mL. A THF (700 mL) solution of BrC_6H_2-2,4,6-*i*-Pr_3 (332.00 g, 1.17 mol) was added dropwise with stirring under steady reflux for 90 min, followed by a 2 h reflux. To the resulting dark-brown solution was added a THF (700 mL) solution of IC_6H_2-2,4,6-Br_3 (147.59 g, 0.335 mol) under steady reflux dropwise over 90 min, followed by a 3.5 h reflux. The mixture was cooled with an ice bath, which resulted in precipitation of a large amount of white solid, and added via a size 12 cannula to an aqueous (500 mL) solution of 150 mL of concentrated HCl under ambient atmosphere in a 5 L three-necked flask, equipped with a mechanical stirrer and a thermometer and cooled with an ice bath, maintaining the temperature below 25 °C. The residual Mg salts were washed with 3 × 50 mL THF, dissolved in 200 mL of water, and added to the acid solution. Anhydrous ether (500 mL) was added to the quenched mixture. The organic layer was decanted off, and the aqueous layer was extracted with another 300 mL of ether, transferred into a 1 L separatory funnel, and extracted with 4 × 100 mL of ether. All organic fractions were combined, reduced in volume to ∼400 mL (using a high vacuum at later stages), and dissolved in 1 L of ether. The ether solution was washed with 500 mL of aqueous Na_2SO_3 (21 g) in three portions and 2 × 100 mL of water, dried with $MgSO_4$, filtered through Celite, and concentrated to 500 mL. The volatile byproducts (ca. 150 mL) were partially removed by a vacuum distillation at 100−120 °C for 4 h and later worked up (flash column chromatography (SiO_2, pentane), Na_2SO_3 wash, distillation) to recover 1,3,5-i-Pr_3-C_6H_3 (117 g, 0.573 mol). The residual brown tar was dissolved in a total of 800 mL of ether, and the solution was filtered through Celite and concentrated to give about 70 g of white crystalline solid in two crops after standing a 0 °C overnight each time. The solid was collected on a frit and washed with cold ether and pentane. The remaining product was dissolved again in a total of 500 mL of pentane and subjected to consecutive flash-column chromatography (SiO_2, pentane) and crystallization at −20 °C to yield another three crops of white crystalline solid, which was collected on a frit and washed with cold pentane each time. All crops were combined and dried under full vacuum at 60 °C for 5 h; yield 102 g (0.182 mol, 54%): ^{1}H NMR ($CDCl_3$, 20 °C) δ 7.35 (d, J_{HH} = 1 Hz, 2H, 4′,6′-*H*), 7.05 (s, 4H, 3,5,3″,5″-*H*), 6.97 (br t, 1H, 2′-*H*), 2.94 (septet, J_{HH} = 6.9 Hz, 2H, 4,4″-C*H*Me_2), 2.70 (septet, J_{HH} = 6.9 Hz, 4H, 2,6,2″,6″-C*H*Me_2), 1.31 (d, J_{HH} = 6.9 Hz, 12 H, 4,4″-CH(C*H*$_3$)$_2$), 1.18 (d, J_{HH} = 6.9 Hz, 12 H, 2,6,2″,6″-CH(C*H*$_3$)$_2$), 1.06 (d, J_{HH} = 6.9 Hz, 12 H, 2,6,2″,6″-CH(C*H*$_3$)$_2$); MS (EI) calcd *m*/*e* 560.3012, found *m*/*e* 560.3039.

***N*-(2,4,6,2″,4″,6″-Hexaisopropyl-[1,1′:3′,1″]terphenyl-5′-yl)-*N*′,N′-bis[2-(2,4,6,2″,4″,6″-hexaisopropyl-[1,1′;3′,1″]terphenyl-5′-ylamino)ethyl]ethane-1,2-diamine (H_3[HIPTN$_3$N])**. A 1 L round-bottom flask equipped with a magnetic stirbar and a Teflon stopcock was charged (inside a nitrogen-filled glovebox) with solid HIPTBr (102.15 g, 0.182 mol) and NaO-*t*-Bu (24.56 g, 98%, 0.250 mol), followed by $N(CH_2CH_2NH_2)_3$ (8.99 g, 97%, 59.6 mmol) and toluene (200 mL). The Pd catalyst solution was prepared by vigorously stirring $Pd_2(dba)_3$ (0.82 g, 0.90 mmol) and *rac*-BINAP (1.70 g, 98%, 268 mmol) in 200 mL of toluene for 3.5 h at room temperature. The mixture was filtered through Celite into the main reaction mixture, and the Celite was rinsed with another 200 mL of toluene. The flask was closed, and the orange mixture was stirred vigorously in an 80 ± 5 °C oil bath for 20 h. Large amounts of NaBr precipitated, and the solution turned dark brown. The precipitate was filtered off under N_2 using Celite, and the volatile components were removed under vacuum. The resulting red foam was dissolved in ether and purified by flash column chromatography on silica in air. The solvents were removed in vacuo to yield an orange foam, which was dissolved in 100 mL of deoxygenated toluene and subjected to a flash column chromatography with deoxygenated toluene (33 cm × 32 cm^2) under dinitrogen. The nearly colorless front fraction was collected under dinitrogen in a 5 L flask (∼2.5 L total) and reduced under high vacuum to 0.5 L. The solution was filtered through Celite under dinitrogen, and the solvents were removed in vacuo to afford a white, amorphous solid after prolonged drying at 65 °C; yield 82.36 g (51.84 mmol, 87%): ^{1}H NMR (C_6D_6, 20 °C) δ 7.22 (s, 12H, 3,5,3″,5″-*H*), 6.54 (br t, 3H, 2′-*H*), 6.45 (br d, 6H, 4′,6′-*H*), 3.60 (t, J_{HH} = 5.0 Hz, 3H, N*H*), 3.17 (septet, J_{HH} = 6.9 Hz, 12H,

(31) Miller, A. R.; Curtin, D. Y. *J. Am. Chem. Soc.* **1976**, *98*, 1860.
(32) Hodgson, H. H.; Mahadevan, A. P. *J. Chem. Soc.* **1947**, 173.
(33) Brookhart, M.; Grant, B.; Volpe, A. F., Jr. *Organometallics* **1992**, *11*, 3920.
(34) Dilworth, J. R.; Richards, R. L. *Inorg. Synth.* **1990**, *28*, 33.
(35) Witanowski, M.; Stefaniak, L.; Szymanski, S.; Januszewski, H. *J. Magn. Reson.* **1977**, *28*, 217.

2,6,2″,6″-C*H*Me$_2$), 2.90 (septet, J_{HH} = 6.9 Hz, 6H, 4,4″-C*H*Me$_2$), 2.80 (q, J_{HH} = 5.1 Hz, 6H, NHC*H*$_2$CH$_2$), 2.20 (approximately t, J_{HH} = 5.1 Hz, 6H, NHCH$_2$C*H*$_2$), 1.31 (d, J_{HH} = 6.9 Hz, 36H, 4,4″-CH(C*H*$_3$)$_2$), 1.27 (d, J_{HH} = 6.9 Hz, 36H, 2,6,2″,6″-CH(C*H*$_3$)$_2$), 1.25 (d, J_{HH} = 6.9 Hz, 36H, 2,6,2″,6″-CH(C*H*$_3$)$_2$); MS (ESI) calcd *m*/*e* 1588.2873 ([M + H]$^+$), found *m*/*e* 1588.2932. Anal. Calcd (found) for $C_{114}H_{162}N_4$: C, 86.19 (86.27); H, 10.28 (10.21); N, 3.53 (3.50).

[HIPTN$_3$N]MoCl. A flame-dried 500 mL round-bottom flask was charged with $MoCl_4(THF)_2$ (9.34 g, 24.45 mmol), H$_3$-[HIPTN$_3$N] (40.00 g, 25.18 mmol), and THF (270 mL), and the resulting dark brown-red solution was stirred vigorously for 1 h. Solid $(Me_3Si)_2NLi$ (12.68 g, 75.78 mmol) was added in portions over a period of 30 min, resulting in a moderate evolution of heat but little color change. The solution was stirred for another 1 h, the solvents were removed in vacuo, and the residue was heated to 60 °C in vacuo. The solid residue was extracted with 4 × 150 mL of pentane, followed by 2 × 200 mL of benzene. The mixture was filtered through Celite and the volume reduced in vacuo to dryness. Crystallization of this crude product from pentane afforded orange solid in several crops, which was collected on a frit, washed with cold pentane, and dried in vacuo at 60 °C; yield 26.56 g (15.45 mmol, 63%): ^{1}H NMR (C_6D_6, 20 °C) δ 11.7 (br s, 6H, 4′,6′-*H*), 7.27 (br s, 12H, 3,5,3″,5″-*H*), 3.20 (br s, 12H, 2,6,2″,6″-C*H*Me$_2$), 2.99 (septet, J_{HH} = 6.6 Hz, 6H, 4,4″-C*H*Me$_2$), 2.27 (s, 3H, 2′-*H*), 1.39 (d, J_{HH} = 4.5 Hz, 36H, 4,4″-CH(C*H*$_3$)$_2$), 1.3 (br s, 72H, 2,6,2″,6″-CH(C*H*$_3$)$_2$), −21.4 (br s, 6H, NC*H*$_2$), −76.3 (br s, 6H, NC*H*$_2$); ^{1}H NMR (CD_2Cl_2, 20 °C) δ 12.0 (br s, 6H, 4′,6′-*H*), 7.00 (br s, 12H, 3,5,3″,5″-*H*), 2.97 (septet, J_{HH} = 6.4 Hz, 6H, 4,4″-C*H*Me$_2$), 2.78 (br s, 12H, 2,6,2″,6″-C*H*Me$_2$), 1.57 (s, 3H, 2′-*H*), 1.32 (d, J_{HH} = 6.0 Hz, 36H, 4,4″-CH(C*H*$_3$)$_2$), 1.09 (br s, 36H, 2,6,2″,6″-CH(C*H*$_3$)$_2$), 0.95 (br sh, 36H, 2,6,2″,6″-CH(C*H*$_3$)$_2$), −16.8 (br s, 6H, NC*H*$_2$), −79.2 (br s, 6H, NC*H*$_2$). Anal. Calcd (found) for $C_{114}H_{159}MoClN_4$: C, 79.75 (79.89); H, 9.33 (9.26); N, 3.26 (3.22); Cl, 2.06 (2.12).

General Procedure for Mg Reduction of MoCl under N$_2$. Two sets of values are given for 0.5−1.0 or 5.0 g (**Mo**Cl) reactions, all of which were carried out inside a N_2-filled glovebox. A 10-fold excess of Mg powder, suspended in THF (2−4 mL/10 mL) in a flame-dried (100 mL/250 mL) round-bottom flask equipped with a glass-coated stirbar, was activated with 0.5 equiv (vs **Mo**Cl) of 1,2-dibromoethane for 15 min. Solid **Mo**Cl was added, followed by 8−12 mL/40 mL of THF, and the resulting mixture was stirred vigorously for a total of 2 h, periodically adjusting the pressure inside the flask to 1 atm. A steady, dark green color usually developed within the first 1 h, and all reductions were complete in 2 h.

[HIPTN$_3$N]MoN═NMgCl(THF)$_3$. Magnesium powder (42 mg, 1.73 mmol) was activated with 0.5 equiv (vs **Mo**Cl) of 1,2-dichloroethane in 2 mL of THF and treated with solid **MoCl** (300 mg, 174.7 μmol), followed by THF (4 mL). The mixture was stirred with a glass-coated stirbar for 2 h, turning very dark green in ∼40 min. The solvents were removed in vacuo, and the residue was dried under vacuum at room temperature for 4 h and extracted with a total of 20 mL of pentane. The combined extracts were filtered through Celite and concentrated to 3 mL in vacuo, leading to precipitation of purple microcrystals, which were isolated by filtration after the mixture, with a few drops of added THF, had stood at −25 °C for several days. The product was rinsed with a small amount of cold pentane and dried for 2 h at RT (room temperature); yield 170 mg (85.6 μmol, 49%): ^{1}H NMR (C_6D_6, 20 °C) δ 7.21 (s, 12H, 3,5,3″,5″-*H*), 7.16 (4′,6′−*H*, obscured), 6.59 (t, 3H, 2′-*H*), 3.77 (br t, 6H, NC*H*$_2$CH$_2$), 3.75 (m, 12 H, OC*H*$_2$), 3.19 (septet, J_{HH} = 6.8 Hz, 12H, 2,6,2″,6″-C*H*Me$_2$), 2.90 (septet, J_{HH} = 6.8 Hz, 6H, 4,4″-C*H*Me$_2$), 2.11 (br t, 6H, NCH$_2$C*H*$_2$), 1.33 (d, J_{HH} = 6.9 Hz, 36H, 4,4″-CH(C*H*$_3$)$_2$), 1.31 (d, J_{HH} = 6.6 Hz, 36H, 2,6,2″,6″-CH(C*H*$_3$)$_2$), 1.22 (d, J_{HH} = 6.6 Hz, 36H, 2,6,2″,6″-CH(C*H*$_3$)$_2$) (OCH$_2$C*H*$_2$ signal is obscured in the 1.3−1.4 ppm region); IR (C_6D_6; cm^{-1}) 1897 (w, sh, ν_{N-N}), 1886 (w, ν_{N-N}), 1812 (minor, ν_{N-N}), 1784 (major, ν_{N-N}), 1755 (minor, ν_{N-N}); IR (C_6D_6 + 10 equiv of THF; cm^{-1}) 1812 (ν_{N-N}), 1785 (w, ν_{N-N}), 1750 (w, sh, ν_{N-N}); IR (Nujol; cm^{-1}) 1898 (w, ν_{N-N}), 1890 (w, ν_{N-N}), 1810 (major, ν_{N-N}), 1782 (minor, ν_{N-N}), 1769 (minor, sh, ν_{N-N}), 1749 (w, sh, ν_{N-N}); IR (DME, 13.5 mM; cm^{-1}) 1857 (ν_{N-N}); IR (THF, 13.5 mM; cm^{-1}) 1856 (A = 7.48, ν_{N-N}), 1811 (A = 2.89, ν_{N-N}). Anal. Calcd (found) for $C_{126}H_{183}ClMgMoN_6O_3$: C, 76.22 (76.18); H, 9.29 (9.27); N, 4.23 (4.16); Cl, 1.79 (1.68).

[HIPTN$_3$N]Mo^{15}N≡^{15}NMgCl(THF)$_3$. A THF (5 mL) solution of **Mo**Cl (250 mg, 145.6 μmol) and Mg powder (35.4 mg, 1.46 mmol) in a 50 mL flask fitted with a Teflon valve was freeze−pump−thaw degassed five times, exposed to $^{15}N_2$ (270 Torr, ∼45 mL, ∼4.5 equiv to **Mo**Cl), and vigorously stirred with a glass-coated stirbar under partial vacuum for 5 h. The resulting dark green solution was worked up under $^{14}N_2$ as described for the unlabeled species to afford a reddish-pink microcrystalline solid; yield 114 mg (57.4 μmol, 39%): ^{1}H NMR (C_6D_6, 20 °C) δ 7.21 (s, 12H, 3,5,3″,5″-H), 7.15 (s, 6H, 4′,6′-*H*), 6.57 (br t, 3H, 2′-*H*), 3.78 (br t, 6H, NC*H*$_2$CH$_2$), 3.77 (m, 12 H, OC*H*$_2$), 3.19 (septet, J_{HH} = 6.8 Hz, 12H, 2,6,2″,6″-C*H*Me$_2$), 2.90 (septet, J_{HH} = 6.8 Hz, 6H, 4,4″-C*H*Me$_2$), 2.11 (br t, 6H, NCH$_2$C*H*$_2$), 1.33 (d, J_{HH} = 7.0 Hz, 36H, 4,4″-CH(C*H*$_3$)$_2$), 1.31 (d, J_{HH} = 6.5 Hz, 36H, 2,6,2″,6″-CH(C*H*$_3$)$_2$), 1.21 (d, J_{HH} = 7.0 Hz, 36H, 2,6,2″,6″-CH(C*H*$_3$)$_2$) (OCH$_2$C*H*$_2$ resonance obscured in the 1.3−1.4 ppm region); ^{15}N NMR (C_6D_6, 20 °C) δ 373 (br s, $^{15}N_\alpha$), 305 (v br, $^{15}N_\beta$); ^{1}H NMR (C_6D_6 + 10 equiv of THF, 20 °C) δ 7.18 (s, 12H, 3,5,3″,5″-*H*), 6.99 (s, 6H, 4′,6′-*H*), 6.50 (br t, 3H, 2′-*H*), 3.81 (t, J_{HH} = 10.5 Hz, 6H, NC*H*$_2$-CH$_2$), 3.65 (m, OC*H*$_2$), 3.16 (br septet, 12H, 2,6,2″,6″-C*H*Me$_2$), 2.87 (septet, J_{HH} = 6.9 Hz, 6H, 4,4″-C*H*Me$_2$), 2.13 (t, J_{HH} = 10.5 Hz, 6H, NCH$_2$C*H*$_2$), 1.35 (obscured, OCH$_2$C*H*$_2$), 1.35 (d, J_{HH} = 6.5 Hz, 36H, 2,6,2″,6″-CH(C*H*$_3$)$_2$), 1.30 (d, J_{HH} = 7.0 Hz, 36H, 4,4″-CH(C*H*$_3$)$_2$), 1.19 (d, J_{HH} = 6.5 Hz, 36H, 2,6,2″,6″-CH(C*H*$_3$)$_2$); ^{15}N NMR (C_6D_6 + 10 equiv of THF, 20 °C) δ 371.0 (d, J($^{15}N_\alpha$−$^{15}N_\beta$) = 10.9 Hz, 1N, $^{15}N_\alpha$), 325.3 (d, J($^{15}N_\alpha$−$^{15}N_\beta$) = 10.3 Hz, 1N, $^{15}N_\beta$); IR (C_6D_6, 42 mM; cm^{-1}) 1834 (w, sh, $\nu^{15}{}_{N-}{}^{15}{}_{N}$), 1824 (w, $\nu^{15}{}_{N-}{}^{15}{}_{N}$), 1753 (major, $\nu^{15}{}_{N-}{}^{15}{}_{N}$), 1725 (major, $\nu^{15}{}_{N-}{}^{15}{}_{N}$), 1698 (minor, $\nu^{15}{}_{N-}{}^{15}{}_{N}$); IR ($C_6D_6$ + 10 equiv of THF; cm^{-1}) 1753 ($\nu^{15}{}_{N-}{}^{15}{}_{N}$), 1724 (w, sh, $\nu^{15}{}_{N-}{}^{15}{}_{N}$); IR (Nujol; cm^{-1}) 1835 (w, $\nu^{15}{}_{N-}{}^{15}{}_{N}$), 1828 (w, $\nu^{15}{}_{N-}{}^{15}{}_{N}$), 1751 (major, $\nu^{15}{}_{N-}{}^{15}{}_{N}$), 1726 (minor, $\nu^{15}{}_{N-}{}^{15}{}_{N}$), 1713 (minor, $\nu^{15}{}_{N-}{}^{15}{}_{N}$), 1692 (w, sh, ν_{N-N}); IR (THF, 13.5 mM; cm^{-1}) 1797 (A = 6.20, $\nu^{15}{}_{N-}{}^{15}{}_{N}$), 1751 ($A$ = 2.43, $\nu^{15}{}_{N-}{}^{15}{}_{N}$). Anal. Calcd (found) for $C_{126}H_{183}ClMgMoN_4{}^{15}N_2O_3$: C, 76.14 (76.21); H, 9.28 (9.19); N, 4.33 (4.26); Cl, 1.78 (1.80).

[Bu$_4$N]{[HIPTN$_3$N]MoN$_2$}. After the reduction of **Mo**Cl (1.0 g, 0.582 mmol) by Mg in THF, 1,4-dioxane (0.5 mL, 5.82 mmol) and Bu_4NCl (194.2 mg, 0.698 mmol) were added and the mixture was stirred for an additional 17 h. The volatile components were removed in vacuo, and the residue was heated at 65 °C in vacuo for 2 h. The residue was extracted with a total of 30 mL of benzene. The extract was filtered through Celite, concentrated to ∼10 mL in vacuo, and layered with 40 mL of pentane. A bright emerald-green amorphous solid formed after standing the solution at room-temperature overnight, which was collected on a frit, washed with pentane, and dried at 60 °C; yield 0.935 g (0.479 mmol, 82%): ^{1}H NMR (C_6D_6, 20 °C) δ 7.64 (br s, 6H, 4′,6′-*H*), 7.23 (s, 12H, 3,5,3″,5″-*H*), 6.35 (br s, 3H, 2′-*H*), 3.96 (br s, 6H, NC*H*$_2$CH$_2$), 3.56 (br s, 12H, 2,6,2″,6″-C*H*Me$_2$), 2.98 (septet, J_{HH} = 6.8 Hz, 6H, 4,4″-C*H*Me$_2$), 2.01 (br s, 8H, NC*H*$_2$CH$_2$CH$_2$CH$_3^+$), 2.01

(obscured, 6H, NCH_2CH_2), 1.42 (d, J_{HH} = 6.6 Hz, 36H, 4,4″-CH(CH_3)$_2$), 1.35 (d, J_{HH} = 6.6 Hz, 36H, 2,6,2″,6″-CH(CH_3)$_2$), 1.28 (br d, J_{HH} = 5.4 Hz, 36H, 2,6,2″,6″-CH(CH_3)$_2$), 0.87 (br m, 8H, $NCH_2CH_2CH_2CH_3^+$), 0.70 (br t, 12H, $NCH_2CH_2CH_2CH_3^+$), 0.70 (obscured, 8H, $NCH_2CH_2CH_2CH_3^+$); IR (C_6D_6; cm^{-1}) 1855 (ν_{N-N}); IR (THF; cm^{-1}) 1859 (ν_{N-N}). Anal. Calcd (found) for $C_{130}H_{195}MoN_7$: C, 79.99 (80.11); H, 10.07 (10.16); N, 5.02 (4.94).

[Bu$_4$N]{[HIPTN$_3$N]Mo^{15}N$_2$}. THF (10 mL) was vacuum-transferred from a dark-purple Na/benzophenone ketyl solution onto a mixture of solid **Mo**Cl (1.5 g, 873.7 μmol) and Mg powder (212 mg, 8.72 mmol) in a 100 mL flask fitted with a Teflon valve. The mixture was freeze−pump−thaw degassed five times, exposed to $^{15}N_2$ (760 Torr, ∼90 mL, ∼4.2 equiv vs **Mo**Cl), and vigorously stirred with a glass-coated stirbar for 6 h. The resulting dark green mixture was treated with Bu_4NCl (291 mg, 1.05 mmol) and 1,4-dioxane (0.74 mL, 8.72 mmol) under an $^{14}N_2$ atmosphere, and the mixture was stirred for an additional 13 h. The solvents were removed in vacuo, and the solid residue was dried in vacuo for 4 h at 60 °C. The residue was extracted with a total of 15 mL of benzene, and the extracts were filtered through Celite, concentrated to 10 mL in vacuo, and layered with 40 mL of pentane. An emerald-green amorphous solid was deposited after 24 h, which was collected by filtration, washed with 25 mL of pentane, and dried at 60 °C for 4 h; yield 1.54 g (788.1 μmol, 90%): ^{1}H NMR (C_6D_6, 20 °C) δ 7.63 (br s, 6H, 4′,6′-*H*), 7.23 (s, 12H, 3,5,3″,5″-*H*), 6.35 (br s, 3H, 2′-*H*), 3.95 (br s, 6H, NCH_2CH_2), 3.55 (br s, 12H, 2,6,2″,6″-C*H*Me$_2$), 2.97 (septet, J_{HH} = 6.8 Hz, 6H, 4,4″-C*H*Me$_2$), 1.99 (br s, 6H, NCH_2CH_2), 1.90 (br s, 8H, NCH_2^+), 1.41 (d, J_{HH} = 6.9 Hz, 36H, 4,4″-CH(CH_3)$_2$), 1.34 (d, J_{HH} = 6.6 Hz, 36H, 2,6,2″,6″-CH(CH_3)$_2$), 1.26 (br d, 36H, 2,6,2″,6″-CH(CH_3)$_2$), 0.80 (approximately quintet, J_{HH} = 6.6 Hz, 8H, $NCH_2CH_2CH_2CH_3^+$), 0.65 (approximately t, J_{HH} = 7.2 Hz, 12H, $NCH_2CH_2CH_2CH_3^+$), 0.59 (obscured, 8H, $NCH_2CH_2CH_2CH_3^+$); ^{15}N NMR (C_6D_6, 20 °C) δ 381 (br s), 367 (br s); IR (C_6D_6; cm^{-1}) 1794 ($\nu_{^{15}N-^{15}N}$). Anal. Calcd (found) for $C_{130}H_{195}MoN_5{}^{15}N_2$: C, 79.91 (80.09); H, 10.06 (9.94); N, 5.12 (5.05).

[Mg(DME)$_3$]$_{0.5}$[MoN$_2$]. A mixture of **Mo**N$_2$ (150 mg, 87.7 μmol) and Mg (21.3 mg, 877 μmol) in DME (3 mL) was vigorously stirred with a glass-coated stirbar for 4 h, turning very dark green in 1 h, filtered through Celite, concentrated to 2 mL, and layered with 5 mL of pentane to yield bright forest-green microcrystals after standing at −25 °C for 3 days. The solid was collected by filtration, washed with 20 mL of pentane−DME (5:1), and dried at 10^{-4} Torr for 1 h at RT, turning dark forest-green; yield 112 mg (60.3 μmol, 69%): ^{1}H NMR (C_6D_6, 20 °C) δ 7.62 (br s, 4′,6′-*H*, [**Mo**N$_2$]$^-$), 7.2 (sh, obscured, 3,5,3″,5″-*H*), 7.17 (s, 3,5,3″,5″-*H*), 7.04 (s, 4′,6′-*H*, [**Mo**N$_2$]{Mg}$^+$), 6.39 (s, 2′-*H*, [**Mo**N$_2$]{Mg}$^+$), 6.28 (br s, 2′-*H*, [**Mo**N$_2$]$^-$), 3.93 (br s, NCH_2CH_2, [**Mo**N$_2$]$^-$), 3.55 (br t, NCH_2CH_2, [**Mo**N$_2$]{Mg}$^+$), 3.55 (obscured, C*H*Me$_2$), 3.19 (s, $MeOCH_2$), 3.01 (s, CH_2OCH_3), 2.99−2.88 (m, obscured, C*H*Me$_2$), 2.19 (br t, NCH_2CH_2, [**Mo**N$_2$]{Mg}$^+$), 1.97 (br s, NCH_2CH_2, [**Mo**N$_2$]$^-$), 1.38 (d, J_{HH} = 6.5 Hz, CH(CH_3)$_2$), 1.33 (d, J_{HH} = 7.0 Hz, CH(CH_3)$_2$), 1.3−1.2 (br, obscured, CH(CH_3)$_2$), 1.17 (d, J_{HH} = 6.5 Hz, CH(CH_3)$_2$), 1.11 (d, J_{HH} = 6.5 Hz, CH(CH_3)$_2$); IR (C_6D_6; cm^{-1}) 1869 (ν_{N-N}, minor), 1854 (ν_{N-N}, major), 1770 (w, sh, ν_{N-N}), 1741 (ν_{N-N}, major); IR (Nujol; cm^{-1}) 1854 (ν_{N-N}), 1790 (w, sh, ν_{N-N}), 1773 (ν_{N-N}), 1749 (ν_{N-N}, minor); IR (THF, 13.5 mM; cm^{-1}) 1853 (A = 6.78, ν_{N-N}), 1808 (A = 1.37, ν_{N-N}). Anal. Calcd (found) for $C_{120}H_{174}Mg_{0.5}MoN_6O_3$: C, 77.62 (77.85); H, 9.45 (9.38); N, 4.53 (4.65); Cl, 0.0 (0.0).

X-ray-quality crystals were obtained by reducing **Mo**Cl with 10 equiv of Mg in DME and layering the resulting dark green, filtered solution with pentane at −25 °C.

[HIPTN$_3$N]MoN$_2$. Following the reduction of **Mo**Cl (5.0 g, 2.91 mmol) by Mg in THF, the dark green THF solution was filtered through Celite and treated with solid $ZnCl_2$ (0.24 g, 1.75 mmol). The color changed to brown, and a gray precipitate of zinc metal formed. The mixture was stirred for an additional 30 min. The solvents were removed in vacuo, and the residue was heated to 60 °C in vacuo. The residue was extracted with a total of 70 mL of pentane. The extracts were filtered through Celite and concentrated in vacuo to yield a green-brown solid in two crops after standing at −25 °C for several days. The product was collected on a frit and dried at 60 °C; yield 3.96 g (2.32 mmol, 80%): ^{1}H NMR (C_6D_6, 20 °C) δ 23.2 (br s, 6H, NCH_2), 6.97 (s, 12H, 3,5,3″,5″-*H*), 2.88 (septet, J_{HH} = 6.6 Hz, 6H, 4,4″-C*H*Me$_2$), 1.93 (br s, 36H, 2,6,2″,6″-CH(CH_3)$_2$), 1.32 (d, J_{HH} = 6.6 Hz, 36H, 4,4″-CH(CH_3)$_2$), 1.13 (br s, 15H, 2,6,2″,6″-C*H*Me$_2$ and 2′-*H*), 0.95 (br s, 36H, 2,6,2″,6″-CH(CH_3)$_2$), −4.8 (br s, 6H, 4′,6′-*H*), −33.5 (br s, 6H, NCH_2); IR (C_6D_6; cm^{-1}) 1990 (ν_{N-N}). Anal. Calcd (found) for $C_{114}H_{159}MoN_6$: C, 80.10 (80.16); H, 9.37 (9.44); N, 4.92 (5.03).

X-ray-quality crystals were grown from a supersaturated pentane solution at RT.

[HIPTN$_3$N]Mo(^{15}N$_2$). THF (0.6 mL) was added to a mixture of [Bu$_4$N][**Mo**^{15}N$_2$] (15 mg) and $ZnCl_2$ (0.8 mg, 0.75 equiv) to give a brown solution and a precipitate of zinc metal rapidly. The volatile components were removed in vacuo, and solid residue was extracted with pentane. The extracts were filtered through Celite, and the solvents were removed in vacuo. The solid residue was dissolved in C_6D_6 and analyzed by IR spectroscopy. IR (C_6D_6; cm^{-1}): 1924 ($\nu^{15}{}_{N-^{15}N}$). The product was found to undergo $^{14}N_2/^{15}N_2$ exchange in solution at ∼22 °C under an atmosphere of $^{14}N_2$ on the time scale of days (18% **Mo**N$_2$ after 6.5 h, 67% after 24.5 h, 88% **Mo**N$_2$ after 95 h, 97% **Mo**N$_2$ after 7 days 5 h).

[HIPTN$_3$N]MoN═NH. Method A. Following the reduction of **Mo**Cl (5.0 g, 2.91 mmol) by Mg in THF, the green THF solution was cooled in a −25 °C freezer for 75 min and titrated dropwise with a cold THF (20 mL) solution of [Et$_3$NH][OTf] (0.732 g, 2.91 mmol) until a steady dark red-brown color was obtained; ∼0.9−0.95 equiv of [Et$_3$NH][OTf] was required. The solvents were removed in vacuo, and the residue was extracted with a total of 125 mL of pentane. The extracts were filtered through Celite and concentrated to 60 mL in vacuo. The mixture was warmed to dissolve any solid, and after several minutes red microcrystals began to form. After standing overnight, the mixture was cooled to −25 °C and the light red-orange crystalline product was collected by filtration in two crops, washed with cold pentane, and dried at 50 °C in vacuo; yield 2.49 g (1.46 mmol, 50%, not optimized): ^{1}H NMR (C_6D_6, 20 °C) δ 8.57 (s, 1H, N═N*H*), 7.27 (br d, 6H, 4′,6′-*H*), 7.19 (s, 12H, 3,5,3″,5″-*H*), 6.63 (br t, 3H, 2′-*H*), 3.66 (br t, 6H, NCH_2CH_2), 3.14 (septet, J_{HH} = 6.7 Hz, 12H, 2,6,2″,6″-C*H*Me$_2$), 2.94 (septet, J_{HH} = 6.9 Hz, 6H, 4,4″-C*H*Me$_2$), 1.96 (br t, 6H, NCH_2CH_2), 1.38 (d, J_{HH} = 6.6 Hz, 36H, 4,4″-CH(CH_3)$_2$), 1.25 (d, J_{HH} = 7.2 Hz, 36H, 2,6,2″,6″-CH(CH_3)$_2$), 1.14 (d, J_{HH} = 6.6 Hz, 36H, 2,6,2″,6″-CH(CH_3)$_2$); IR (C_6D_6; cm^{-1}) 3135 (ν_{N-H}), 1587 (ν_{N-N}), 1137 (ν_{N-N-H}); IR (Nujol; cm^{-1}) 3134 (ν_{N-H}), 1587 (ν_{N-N}), 1137 (ν_{N-N-H}). Anal. Calcd (found) for $C_{114}H_{160}MoN_6$: C, 80.05 (79.88); H, 9.43 (9.36); N, 4.91 (5.04).

Method B (Preferred). An ether (6 mL) solution of [Et$_3$NH][BAr′$_4$] (234.0 mg, 242.4 μmol) was cooled to −25 °C and treated with solid [Bu$_4$N][**Mo**N$_2$] (450 mg, 230.5 μmol), while the solution was stirred with a glass-coated stirbar. A dark orange solution was produced in minutes. The solution was stirred for an additional 10 min at RT, and the volatile components were removed in vacuo. The residue was exposed to a high vacuum at 40 °C for 2 h and extracted with a total of 40 mL of pentane. The extracts were filtered

through Celite, and the solvents were removed in vacuo. The resulting light orange solid was treated with ~7 mL of Me_4Si. Upon shaking of the sample, a homogeneous solution was obtained, in which fine light orange microcrystals began forming in a few minutes. After the mixture was standing overnight at −25 °C, the solid was collected by filtration, washed with a total of 20 mL of cold Me_4Si, and dried at 50 °C for 10 h in vacuo; yield 264 mg (154 μmol, 67%).

An analogous procedure was used to prepare **Mo**N═NH with 0.9 equiv of $[Et_3NH][BAr'_4]$, except that the product was recrystallized two more times from Me_4Si, as described above.

[HIPTN$_3$N]Mo^{15}N═^{15}NH. An ether solution (6 mL) of $[Et_3NH][BAr'_4]$ (217.4 mg, 225.2 μmol) was treated with solid $[Bu_4N][\mathbf{Mo}^{15}N_2]$ (400 mg, 204.7 μmol) at −25 °C while stirring the solution with a glass-coated stirbar to produce a dark orange solution in minutes. The solution was stirred for an additional 10 min, and the volatile components were removed in vacuo. The solid residue was dried under vacuum for 3 h at RT and extracted with a total of 40 mL of pentane; the extracts were filtered through Celite and brought to dryness. The resulting light orange solid was recrystallized from Me_4Si at −25 °C to yield a light orange microcrystalline solid in two crops, which was isolated by filtration, washed with cold Me_4Si, and dried at 50 °C for 3 h in vacuo; yield 252 mg (147.2 μmol, 72%): ^{1}H NMR (C_6D_6, 20 °C) δ 8.57 (dd, $^1J(^{15}N_\beta-H) = 53.6$ Hz, $^2J(^{15}N_\alpha-H) = 7.9$ Hz, 1H, $^{15}N_\alpha=^{15}N_\beta H$), 7.27 (s, 6H, 4′,6′-*H*), 7.19 (s, 12H, 3,5,3″,5″-*H*), 6.62 (br t, 3H, 2′-*H*), 3.65 (br t, 6H, NCH_2CH$_2$), 3.14 (septet, $J_{HH} = 6.7$ Hz, 12H, 2,6,2″,6″-C*H*Me$_2$), 2.93 (septet, $J_{HH} = 6.8$ Hz, 6H, 4,4″-C*H*Me$_2$), 1.95 (br t, 6H, NCH_2CH$_2$), 1.37 (d, $J_{HH} = 6.9$ Hz, 36H, 4,4″-CH(CH_3)$_2$), 1.24 (d, $J_{HH} = 6.9$ Hz, 36H, 2,6,2″,6″-CH(CH_3)$_2$), 1.13 (d, $J_{HH} = 6.6$ Hz, 36H, 2,6,2″,6″-CH(CH_3)$_2$); ^{15}N NMR (C_6D_6, 20 °C) δ 409.0 (dd, $J(^{15}N_\alpha-^{15}N_\beta) = 15.7$ Hz, $^2J(^{15}N_\alpha-H) = 7.7$ Hz, 1N, $^{15}N_\alpha = ^{15}N_\beta H$), 232.6 (dd, $^1J(^{15}N_\beta-H) = 53.3$ Hz, $J(^{15}N_\alpha-^{15}N_\beta) = 16.1$ Hz, 1N, $^{15}N_\alpha=^{15}N_\beta H$); IR ($C_6D_6$; cm^{-1}) 3129 ($\nu_{^{15}N_\beta-H}$), 1523 ($\nu_{^{15}N-^{15}N}$), 1125 ($\nu_{^{15}N-^{15}N-H}$); IR (Nujol; cm^{-1}) 3129 ($\nu_{^{15}N_\beta-H}$), 1524 ($\nu_{^{15}N-^{15}N}$), 1125 ($\nu_{^{15}N-^{15}N-H}$). Anal. Calcd (found) for $C_{114}H_{160}MoN_4{}^{15}N_2$: C, 79.96 (79.77); H, 9.42 (9.56); N, 5.02 (4.86).

[HIPTN$_3$N]MoH. MoN═NH (300 mg, 175.4 μmol), prepared by the method shown in eq 7 (method A; vide supra), was heated in 6 mL of heptane with vigorous stirring for a total of 97 h, at which time essentially no **Mo**N═NH remained according to ^{1}H NMR spectra of an aliquot. The product **Mo**H started to precipitate shortly after all **Mo**N═NH had dissolved. After 97 h the bright brick-red solid was collected by filtration, washed with pentane, and combined with another crop of solid that was obtained by standing the concentrated filtrate at −25 °C overnight. The solid was extracted with benzene, and the extracts were filtered through Celite. The solvent was removed in vacuo, and the resulting solid was treated with 10 mL of pentane to yield a homogeneous solution, from which fine brick-red microcrystalline solid rapidly began precipitating. After the solution was kept at −25 °C overnight, the solid was collected by filtration, washed with cold pentane, and dried in vacuo at 60 °C for 2 h; yield 182 mg (108 μmol, 62%): ^{1}H NMR (C_6D_6, 20 °C) δ 7.26 (br s, 12H, 3,5,3″,5″-*H*), 3.26 (br s, 12H, 2,6,2″,6″-C*H*Me$_2$), 2.92 (br septet, $J_{HH} = 6.6$ Hz, 6H, 4,4″-C*H*Me$_2$), 1.91 (s, 3H, 2′-*H*), 1.35 (d, $J_{HH} = 6.6$ Hz, 36H, 4,4″-CH(CH_3)$_2$), 1.29 (br s, 36H, 2,6,2″,6″-CH(CH_3)$_2$), 0.98 (v br s, 36H, 2,6,2″,6″-CH(CH_3)$_2$), the 4′,6′-H and N−CH$_2$ resonances are not observed; IR (C_6D_6; cm^{-1}) 1748 (ν_{Mo-H}). Anal. Calcd (found) for $C_{114}H_{160}MoN_4$: C, 81.38 (81.46); H, 9.59 (9.51); N, 3.33 (3.40).

The deuteride derivative was prepared by subjecting a degassed solution of **Mo**H in C_6D_6 to 1 atm of D_2 for 24 h. IR (C_6D_6; cm^{-1}): 1252 (ν_{Mo-D}).

{[HIPTN$_3$N]Mo═NNH$_2$}[BAr′$_4$]. An Et_2O (5 mL) solution of **Mo**N═NH (250 mg, 146.2 μmol) was treated with solid $[H(OEt_2)_2][BAr'_4]$ (153.9 mg, 152.0 μmol) with stirring over a period of 1.5 h to give a dark red-brown solution. Volatiles were removed in vacuo, and the solid residue was extracted with pentane. The extracts were filtered through Celite and brought to dryness in vacuo. The resulting dark red amorphous solid was dried at 55 °C for 2 h; yield 255 mg (99.0 μmol, 68%): ^{1}H NMR (C_6D_6, 20 °C) δ 8.36 (br s, 8H, C_6H_3-3,5-(CF$_3$)$_2$), 7.66 (br s, 4H, C_6H_3-3,5-(CF$_3$)$_2$), 7.13 (s, 12H, 3,5,3″,5″-*H*), 6.80 (br s, 6H, 4′,6′-*H*), 6.66 (s, 2H, N−NH_2), 6.61 (br t, 3H, 2′-*H*), 3.64 (br t, 6H, NCH_2CH$_2$), 2.89 (septet, $J_{HH} = 6.8$ Hz, 6H, 4,4″-C*H*Me$_2$), 2.67 (septet, $J_{HH} = 6.6$ Hz, 12H, 2,6,2″,6″-C*H*Me$_2$), 2.28 (br t, 6H, NCH$_2$CH_2), 1.33 (d, $J_{HH} = 6.9$ Hz, 36H, 4,4″-CH(CH_3)$_2$), 1.10 (d, $J_{HH} = 6.9$ Hz, 36H, 2,6,2″,6″-CH(CH_3)$_2$), 0.98 (d, $J_{HH} = 6.9$ Hz, 36H, 2,6,2″,6″-CH-(CH_3)$_2$); ^{19}F NMR (C_6D_6, 20 °C) δ −61.8 (s, CF$_3$); IR (C_6D_6; cm^{-1}) 3379 (ν_{N-H}), 3274 (ν_{N-H}). Anal. Calcd (found) for $C_{146}H_{173}BF_{24}MoN_6$: C, 68.11 (68.26); H, 6.77 (6.84); N, 3.26 (3.14). The compound readily crystallizes from pentane when seeded with a small amount of crystalline sample, originally obtained by prolonged storage of a pentane solution at −25 °C in a vial closed with a Teflon-lined cap, which appears to initiate crystallization.

{[HIPTN$_3$N]Mo═^{15}N^{15}NH$_2$}[BAr′$_4$]). Ether (0.6 mL) was added to a mixture of solid **Mo**^{15}N═^{15}NH (40 mg) and $[H(OEt_2)_2][BAr'_4]$ (23.6 mg, 1 equiv). After 1 h the solvent was removed in vacuo and the dark red residue was dissolved in C_6D_6 for spectroscopic analysis: ^{1}H NMR (C_6D_6, 20 °C) δ 6.67 (dd, $^1J(^{15}N_\beta-H) = 90.5$ Hz, $^2J(^{15}N_\alpha-H) = 1.4$ Hz, $^{15}N_\alpha-^{15}N_\beta H_2$) (other resonances identical to those measured for the unlabeled sample); ^{15}N NMR (C_6D_6, 20 °C) δ 357.5 (d, $J(^{15}N_\alpha-^{15}N_\beta) = 11.4$ Hz, 1N, $^{15}N_\alpha=^{15}N_\beta H_2$), 140.0 (td, $^1J(^{15}N_\beta-H) = 90.4$ Hz, $J(^{15}N_\alpha-^{15}N_\beta) = 11.0$ Hz, 1N, $^{15}N_\alpha = ^{15}N_\beta H_2$); IR ($C_6D_6$; cm^{-1}) 3370 ($\nu_{^{15}N-H}$), 3270 ($\nu_{^{15}N-H}$).

[HIPTN$_3$N]Mo≡N. A toluene (70 mL) solution of **Mo**Cl (5.0 g, 2.91 mmol) and Me_3SiN_3 (0.8 mL, 97%, 5.82 mmol) in a 100 mL flask fitted with a Teflon valve was stirred closed in a 90 °C oil bath for 65 h, after which time no **Mo**Cl could be discerned by ^{1}H NMR of an aliquot. The solvents were removed from the dark yellow-brown solution, and the residue was dried at 90 °C and extracted with a total of 700 mL of pentane. The extracts were filtered through Celite and concentrated in vacuo to yield (at −25 °C) bright yellow solid in three crops, which was collected by filtration, washed with cold pentane, and dried at 80 °C; yield 3.79 g (2.24 mmol, 77%): ^{1}H NMR (C_6D_6, 20 °C) δ 7.94 (br s, 6H, 4′,6′-*H*), 7.20 (s, 12H, 3,5,3″,5″-*H*), 6.60 (s, 3H, 2′-*H*), 3.55 (br t, 6H, NCH_2CH$_2$), 3.10 (septet, $J_{HH} = 6.5$ Hz, 12H, 2,6,2″,6″-C*H*Me$_2$), 2.93 (septet, $J_{HH} = 6.8$ Hz, 6H, 4,4″-C*H*Me$_2$), 1.79 (br t, 6H, NCH$_2$CH_2), 1.36 (d, $J_{HH} = 6.6$ Hz, 36H, 4,4″-CH(CH_3)$_2$), 1.23 (d, $J_{HH} = 6.9$ Hz, 36H, 2,6,2″,6″-CH(CH_3)$_2$), 1.09 (br d, $J_{HH} = 6.0$ Hz, 36H, 2,6,2″,6″-CH(CH_3)$_2$); IR (C_6D_6; cm^{-1}) 1013 (ν_{Mo-N}). Anal. Calcd (found) for $C_{114}H_{159}MoN_5$: C, 80.76 (80.66); H, 9.45 (9.39); N, 4.13 (4.17).

X-ray-quality crystals were grown from a supersaturated pentane solution at 22 °C.

[HIPTN$_3$N]Mo≡N (50% ^{15}N Labeled). A mixture of **Mo**Cl (0.5 g, 0.291 mmol), NaN_3(1-^{15}N) (29 mg, 0.439 mmol), and TMEDA (220 μL, 1.455 mmol) in benzene (10 mL) was vigorously stirred in a closed system at 75 °C for 49 h. The solvents were removed in vacuo, and the solid residue was recrystallized three times from pentane to yield a yellow crystalline solid, which was isolated by filtration and dried in vacuo; yield 60 mg (35.4 μmol, 12%, not optimized): ^{1}H NMR (C_6D_6, 20 °C) δ 7.95 (br s, 6H, 4′,6′-*H*), 7.21 (s, 12H, 3,5,3″,5″-*H*), 6.60 (s, 3H, 2′-*H*), 3.55 (br t, 6H, NCH_2-CH$_2$), 3.10 (septet, $J_{HH} = 6.5$ Hz, 12H, 2,6,2″,6″-C*H*Me$_2$), 2.93

(septet, J_{HH} = 6.8 Hz, 6H, 4,4″-C*H*Me$_2$), 1.77 (br t, 6H, NCH$_2$C*H*$_2$), 1.36 (d, J_{HH} = 6.6 Hz, 36H, 4,4″-CH(C*H*$_3$)$_2$), 1.23 (d, J_{HH} = 6.9 Hz, 36H, 2,6,2″,6″-CH(C*H*$_3$)$_2$), 1.09 (br d, J_{HH} = 6.0 Hz, 36H, 2,6,2″,6″-CH(C*H*$_3$)$_2$); ^{15}N NMR (C_6D_6, 20 °C) δ 898.2 (Mo≡^{15}*N*); IR (C_6D_6; cm^{-1}) 1012 ($\nu_{Mo-^{14}N}$), 986 ($\nu_{Mo-^{15}N}$). Anal. Calcd (found) for $C_{114}H_{159}MoN_{4.5}{}^{15}N_{0.5}$: C, 80.73 (80.68); H, 9.45 (9.54); N, 4.16 (4.21).

{[HIPTN$_3$N]Mo=NH}[BAr′$_4$]. An ether solution (5 mL) of **Mo**≡N (250 mg, 147.4 μmol) was treated with solid [H(OEt$_2$)$_2$][BAr′$_4$] (155.3 mg, 153.4 μmol) at −25 °C with stirring to give a dark red-brown solution. The mixture was allowed to warm to RT and was stirred for 1 h. Volatile components were removed in vacuo, and the solid residue was extracted with pentane. The extract was filtered through Celite and taken to dryness in vacuo. The resulting dark red amorphous solid was dried at 65 °C for 2 h; yield 350 mg (136.7 μmol, 93%): ^{1}H NMR (C_6D_6, 20 °C) δ 8.36 (br s, 8H, C$_6$*H*$_3$-3,5-(CF$_3$)$_2$), 7.65 (br s, 4H, C$_6$*H*$_3$-3,5-(CF$_3$)$_2$), 7.15 (s, 12H, 3,5,3″,5″-*H*), 6.88 (s, 6H, 4′,6′-*H*), 6.60 (s, 1H, N*H*$^+$), 6.55 (s, 3H, 2′-*H*), 3.69 (br t, 6H, NC*H*$_2$CH$_2$), 2.89 (septet, J_{HH} = 6.8 Hz, 6H, 4,4″-C*H*Me$_2$), 2.64 (septet, J_{HH} = 6.8 Hz, 12H, 2,6,2″,6″-C*H*Me$_2$), 2.23 (br t, 6H, NCH$_2$C*H*$_2$), 1.34 (d, J_{HH} = 6.6 Hz, 36H, 4,4″-CH(C*H*$_3$)$_2$), 1.15 (d, J_{HH} = 6.9 Hz, 36H, 2,6,2″,6″-CH(C*H*$_3$)$_2$), 1.00 (d, J_{HH} = 6.6 Hz, 36H, 2,6,2″,6″-CH(C*H*$_3$)$_2$); ^{19}F NMR (C_6D_6, 20 °C) δ −62.5 (s, CF$_3$); IR (C_6D_6; cm^{-1}) 3341 (ν_{N-H}). Anal. Calcd (found) for $C_{146}H_{172}BF_{24}MoN_5$: C, 68.51 (68.39); H, 6.77 (6.73); N, 2.74 (2.80).

The compound readily crystallizes from pentane when seeded with a small amount of crystalline sample, originally obtained by prolonged storage of a pentane solution at −25 °C in a vial closed with a Teflon-lined cap, which appears to initiate crystallization.

{[HIPTN$_3$N]Mo=NH}[BAr′$_4$] (50% ^{15}N Labeled). Ether (0.6 mL) was added to a mixture of solid **Mo**≡$^{15/14}$N (30 mg) and [H(OEt$_2$)$_2$][BAr′$_4$] (17.9 mg, 1 equiv). After 1 h the ether was removed in vacuo and the residue was dissolved in C_6D_6 for spectroscopic analysis: ^{1}H NMR (C_6D_6, 20 °C) δ 6.60 (br s, 0.5 H, Mo=^{14}N*H*), 6.59 (d, $^1J(^{15}N-H)$ = 73.7 Hz, 0.5 H, Mo=^{15}N*H*) (other resonances identical with those measured for the unlabeled sample); ^{15}N NMR (C_6D_6, 20 °C) δ 427.7 (d, $^1J(^{15}N-H)$ = 74 Hz, Mo≡^{15}*N*H); IR (C_6D_6; cm^{-1}) 3340 ($\nu_{^{14}N-H}$), 3334 ($\nu_{^{15}N-H}$).

{[HIPTN$_3$N]Mo(NH$_3$)}[BPh$_4$]. Ammonia (100 mL, 220 Torr, ca. 4 equiv to **Mo**Cl) was vacuum-transferred from a bronze-colored solution of Na onto a frozen CH_2Cl_2 (7 mL) solution of **Mo**Cl (0.5 g, 0.291 mmol) and NaBPh$_4$ (110 mg, 0.321 mmol). The mixture was thawed and stirred at RT for 1 h under partial vacuum; the solution turned dark red, and a fine white precipitate formed. The volatile components were removed in vacuo, and the solid residue was recrystallized from pentane to yield a red-brown semiamorphous solid, which was collected by filtration, washed with pentane, and dried at 55 °C; yield 420 mg (0.208 mmol, 71%): ^{1}H NMR (C_6D_6, 20 °C) δ 7.82 (br s, 8H, B(C$_6$*H*$_5$)), 7.16 (s, 12H, 3,5,3″,5″-*H*), 7.16−7.00 (obscured, 12 H, B(C$_6$*H*$_5$)), 2.92 (br septet, 12H, 2,6,2″,6″-C*H*Me$_2$), 2.8 (v br s, 6H, 4,4″-C*H*Me$_2$), 1.34 (d, J_{HH} = 6.0 Hz, 36H, 4,4″-CH(C*H*$_3$)$_2$), 1.18 (br s, 36H, 2,6,2″,6″-CH(C*H*$_3$)$_2$), 1.04 (v br s, 36H, 2,6,2″,6″-CH(C*H*$_3$)$_2$), −0.6 (s, 3H, 2′-*H*), −21 (br s, 6H, NC*H*$_2$), −103 (br s, 6H, NC*H*$_2$) (the 4′,6′-*H* resonance is strongly broadened and obscured in the 10−5 ppm region); ^{1}H NMR (CD_2Cl_2, 20 °C) δ 7.23 (br s, 8H, B(C$_6$*H*$_5$)), 6.97 (s, 12H, 3,5,3″,5″-*H*), 6.97 (obscured, 8 H, B(C$_6$*H*$_5$)), 6.82 (br s, 4H, B(C$_6$*H*$_5$)), ∼6 (v br, 4′,6′-*H*), 2.98 (br septet, 12H, 2,6,2″,6″-C*H*Me$_2$), 2.63 (br s, 6H, 4,4″-C*H*Me$_2$), 1.32 (d, J_{HH} = 6.6 Hz, 36H, 4,4″-CH(C*H*$_3$)$_2$), 1.07 (br s, 36H, 2,6,2″,6″-CH(C*H*$_3$)$_2$), 0.9 (v br s, 36H, 2,6,2″,6″-CH(C*H*$_3$)$_2$), −4.1 (s, 3H, 2′-*H*),-18 (br s, 6H, NC*H*$_2$), −106 (br s, 6H, NC*H*$_2$). Anal. Calcd (found) for $C_{138}H_{182}BMoN_5$: C, 82.15 (82.25); H, 9.09 (9.15); N, 3.47 (3.59).

{[HIPTN$_3$N]Mo(NH$_3$)}[BAr′$_4$]. A procedure analogous to that used for the synthesis of [**Mo**(NH$_3$)][BPh$_4$] was followed, starting from **Mo**Cl (200 mg, 116.5 μmol), NaBAr′$_4$ (114 mg, 128.6 μmol), and NH$_3$ (50 mL, 175 Torr, ca. 4 equiv to **Mo**Cl), except that the product was isolated by removal of volatiles from filtered pentane extracts and drying of the resulting red-brown solid in vacuo at 55 °C; yield 240 mg (93.7 μmol, 80%): ^{1}H NMR (C_6D_6, 20 °C): δ 8.27 (br s, 8H, C$_6$*H*$_3$-3,5-(CF$_3$)$_2$), 7.63 (br s, 4H, C$_6$*H*$_3$-3,5-(CF$_3$)$_2$), 7.16 (s, 12H, 3,5,3″,5″-*H*), 2.93 (br septet, 12H, 2,6,2″,6″-C*H*Me$_2$), 2.7 (v br s, 6H, 4,4″-C*H*Me$_2$), 1.35 (d, J_{HH} = 6.3 Hz, 36H, 4,4″-CH(C*H*$_3$)$_2$), 1.19 (br s, 36H, 2,6,2″,6″-CH(C*H*$_3$)$_2$), 1.0 (v br s, 36H, 2,6,2″,6″-CH(C*H*$_3$)$_2$), −2.6 (s, 3H, 2′-*H*), −21 (br s, 6H, NC*H*$_2$), −103 (br s, 6H, NC*H*$_2$) (the 4′,6′-*H* signal is strongly broadened and obscured in the 10−5 ppm region); ^{1}H NMR (CD_2Cl_2, 20 °C) δ 7.72 (br s, 8H, C$_6$*H*$_3$-3,5-(CF$_3$)$_2$), 7.56 (br s, 4H, C$_6$*H*$_3$-3,5-(CF$_3$)$_2$), 6.97 (s, 12H, 3,5,3″,5″-*H*), 2.97 (br sept, 12H, 2,6,2″,6″-C*H*Me$_2$), 2.64 (v br s, 6H, 4,4″-C*H*Me$_2$), 1.31 (d, J_{HH} = 6.6 Hz, 36H, 4,4″-CH(C*H*$_3$)$_2$), 1.08 (br s, 36H, 2,6,2″,6″-CH(C*H*$_3$)$_2$), 0.94 (v br s, 36H, 2,6,2″,6″-CH(C*H*$_3$)$_2$), −4.7 (s, 3H, 2′-*H*), −17 (br s, 6H, NC*H*$_2$), −103 (br s, 6H, NC*H*$_2$) (the 4′,6′-*H* signal is strongly broadened and obscured in the 4−7 ppm region); ^{19}F NMR (C_6D_6, 20 °C) δ −61.5 (s, CF$_3$). Anal. Calcd (found) for $C_{146}H_{174}BF_{24}MoN_5$: C, 68.45 (68.37); H, 6.85 (6.79); N, 2.73 (2.78). The product readily crystallizes from pentane solution as bright red prisms, sparingly soluble in pentane (76% recovery of 0.5 g after standing for overnight at −25 °C), when the solution is seeded with a trace amount of the crystalline sample. The original crystalline sample was obtained from a concentrated pentane solution of the crude product, synthesized with rigorous exclusion of air and moisture, after standing at −25 °C for several days.

X-ray-quality crystals were grown from a supersaturated pentane solution at RT.

{[HIPTN$_3$N]Mo(^{15}NH$_3$)}[BAr′$_4$]. A procedure analogous to that used for the synthesis of [**Mo**(NH$_3$)][BAr′$_4$] was followed, starting from **Mo**Cl (300 mg, 174.7 μmol), NaBAr′$_4$ (170.3 mg, 192.2 μmol), and ^{15}NH$_3$ (61 mL, 180 Torr, ∼3.4 equiv vs **Mo**Cl); yield 396 mg (155 μmol, 88%). Spectroscopic data are identical with those of unlabeled [**Mo**(NH$_3$)][BAr′$_4$]. Anal. Calcd (found) for $C_{146}H_{174}BF_{24}MoN_4{}^{15}N$: C, 68.43 (68.27); H, 6.84 (6.80); N, 2.77 (2.68).

X-ray Crystallography. X-ray data were collected on Bruker Smart diffractometers equipped with CCD area detector and Mo Kα X-ray source; an Apex CCD detector was used in the case of **Mo**≡N and {**Mo**(NH$_3$)}{BAr′$_4$} structures. All structures were solved and refined using Bruker SHELXTL 5.1. Crystals of essentially all [HIPTN$_3$N]Mo derivatives obtained from pentane are heavily solvated; pentane of crystallization is identifiable by ^{1}H NMR, and prolonged heating under vacuum is typically required to obtain solvent-free solids. In view of this, electron density peaks that were present in void areas of every structure discussed here and that could not be modeled as discrete molecules were assigned to *n*-pentane of solvation (1.2−4.5 equiv of *n*-pentane/Mo as suggested by SQUEEZE[36]). In all cases final stages of refinement were done on solvent-free modified structure factors generated by SQUEEZE.

Acknowledgment. R.R.S. is grateful to the National Institutes of Health (Grant GM 31978) for research support.

(36) (a) van der Sluis, P.; Spek, A. L. *Acta Crystallogr.* **1990**, *A46*, 194−201. (b) Spek, A. L. *Acta Crystallogr.* **1990**, *A46*, C-34.

We thank Prof. S. J. Lippard for use of his diffractometer to collect data using the Apex detector and Dmitry V. Khoroshun for sharing computational results on related model systems and for fruitful discussions.

Supporting Information Available: Crystal and structure refinement data, atomic coordinates and equivalent isotropic displacement parameters, bond lengths and angles, anisotropic displacement parameters, hydrogen coordinates and isotropic displacement parameters, and torsion angles for all crystallographically characterized compounds. This material is available free of charge via the Internet at http://pubs.acs.org.

IC020505L